et al., 1998; Marmorstein *et al.*, 1998; Zhang *et al.*, 1998; Linke *et al.*, 2003; Sengupta *et al.*, 2003) and inhibits the Rad51-dependent HR (Cromie *et al.*, 2001; Linke *et al.*, 2003). When DSBs were induced, the association of p53 and Rad51 was prevented by an unknown mechanism. As the reduction of Rad51 and p53 interaction was also observed after irradiation (Figure 3c), it is likely that the Vpr-activated DNA-damage signaling overlaps with the cellular signals evoked by irradiation.

Biological relevance of Vpr-induced DSBs and HR for HIV-1 infection

Vpr expression enhances the rate of HR, but several reports suggest that NHEJ rather than HR contributes to viral infection (Daniel *et al.*, 1999; Li *et al.*, 2001; Jeanson *et al.*, 2002; Lau *et al.*, 2005). Additionally, Rad52, a cellular component of HR, was shown to work as a suppressive factor for HIV-1 transduction (Lau *et al.*, 2004). Together with data that the deletion of genes involved in HR, such as XRCC2 or XRCC3, did not alter the rate of viral integration (Chan *et al.*, 2004), it seems that upregulation of HR by Vpr does not by itself contribute to viral transduction.

In contrast, chemical compounds that generate DSBs increase the rate of integration of viral DNA into the host genome (Groschel and Bushman, 2005). This phenomenon has been explained by delayed progression at the G2/M phase due to DSBs. Additionally, caffeine and caffeine-related methylxanthines are known to impair HIV-1 infection (Nunnari *et al.*, 2005), and an ATM inhibitor, KU55933, is known to decrease the integration of viral DNA into host genome (Lau *et al.*, 2005). These observations suggest that a DSB-induced cellular signal, not HR, is important for viral integration, and that Vpr-induced DSB contributes to efficient viral integration in an ATM-dependent manner. An important issue to clarify is how cellular signals activated by ATM contribute to increased viral integration.

Possible mechanism of Vpr-induced DSBs and cell cycle abnormality

The mechanism of Vpr-induced DSBs is presently obscure. In the previous work, we showed that DSBs are induced by incubating isolated nuclei with purified recombinant Vpr protein (Tachiwana *et al.*, 2006). A purified Vpr possessed DNA binding activity, but it did not show any nuclease activity or activity of nicking DNAs. Additionally, Vpr is present in the chromatin fraction (Ishizaka, unpublished results, Lai *et al.*, 2005), implying the possibility that Vpr induces DSBs by modifying a chromatin structure to allow nucleases easy access. Another possibility is that Vpr associates with uncharacterized nuclease and recruits its activity to the vicinity of chromosomes. Studies are ongoing to identify cellular factor(s) that facilitate recruitment of Vpr to chromatin and induction of DSBs.

It is commonly accepted that Vpr-induced cell cycle abnormality is observed at the G2/M phase but not at the G1/S phase (Mahalingam *et al.*, 1998). Actually, we observed cellular accumulation at the G2/M phase in MIT-23 cells when Vpr expression was initiated (Shimura *et al.*, 1999b). Our present observation on the activation of ATM-dependent signal pathway by Vpr envisages that Vpr-induced cell cycle abnormality depends on ATM activation. A recent study, however, has shown that the ATR–Chk1 pathway, but not ATM–Chk2, is necessary for Vpr-induced G2 arrest (Roshal *et al.*, 2003; Zimmerman *et al.*, 2004). One possible explanation is that DSB-induced G2 arrest, for example, by X-ray irradiation largely depends on ATR-dependent signaling (Brown and Baltimore, 2003). The molecular linkage between ATM activation by Vpr and Vpr-induced cell cycle abnormality, however, needs to be carefully investigated.

Impact of Vpr-induced DSBs on the mechanism of tumor development in HIV-1-positive patients

We showed that DSBs and an increased rate of HR were induced when rVpr was added to the culture medium exogenously (Figure 6). Recently, we also found that Vpr is present in serum of HIV-1-positive patients (Levy *et al.*, 1994) at the concentration of about 0.7 nM (Hoshino *et al.*, submitted). In the current study, we used 3.7 nM of rVpr to obtain the definite activity inducing DSBs, but it would be possible that the high concentration of Vpr is present in the foci of HIV-1 infection, suggesting that DSBs can be generated in the cells within HIV-1-positive patients. The finding that Vpr is present in serum impacts the understanding of the mechanism of tumor development in HIV-1 positive patients. As reported by Biggar *et al.*, the relative risk of

Figure 6 Increased rate of intrachromosomal HR after treatment with rVpr. (**a**) Focus formation of γ-H2AX in cells treated with or without rVpr. HT1080 cells were incubated for 48 h in the presence of 3.7 nM of rVpr (see Materials and methods section), and subjected to immunohistochemical analysis by antibodies against ATM-p and γ-H2AX. Effects of KU55933 on rVpr-induced focus formation of these molecules are shown. As controls, the effects of the same concentration of GST, as an irrelevant bacteria-derived recombinant protein, are depicted (right panel). Their signals are shown as red spots in the nucleus (blue). (**b**) Effects of rVpr on HR. HT/DR–GFP cells (clone-1) were infected with Adβgal or Ad–SceI–NG with or without the addition of 3.7 nM of rVpr (middle panel). As a control, the same amount of GST was added to the culture (right panel). A region where no GFP-positive cells were present in control sample was first determined (upper left panel). Then numbers of cells in the gated areas were counted in the specimens after viral infection with or without treatment of recombinant proteins. (**c**) Vpr-induced increase of HR depends on ATM. Data obtained in Figure 6b were summarized (left panel). The addition of rVpr reproducibly enhanced the number of GFP-positive cells ($P<0.01$). Effects of ATM inhibitor (ATMi) were analysed by the same procedures shown in Figure 6b (right panel). KU55933 (ATMi) was added at a concentration of 1 mM at the same time that rVpr was added. As a control, the corresponding amount of dimethylsulfoxide (final concentration: 0.1% volume), which was used as a solvent for the compound, was included. ATMi significantly inhibited the rate of HR ($P<0.01$).

malignancy in AIDS patients was estimated to be 60- to1000-fold higher than healthy controls (Mayer *et al.*, 1995; Biggar *et al.*, 1996; Straus, 2001). Although it has been thought that an impaired cellular immunity under AIDS conditions permits the development of tumorigenesis (Knowles, 2003), recent observations indicate that non-AIDS-defining malignancies, tumors found in HIV-1-positive patients who have no deteriorated cellular immunity, are frequently observed in HIV-1-positive patients (Herida *et al.*, 2003; Burgi *et al.*, 2005; Lim and Levine, 2005). As antiretroviral therapy can effectively protect patients from severe infectious diseases (Chadburn and Cesarman, 1997; Elenitoba-Johnson and Jaffe, 1997), development of malignant tumors will be a critical prognostic factor of HIV-1 positive patients in the future. More precise study is required to clarify the molecular linkage of Vpr and malignant transformation.

Materials and methods

Cell culture and establishment of HT/DR-GFP

HT1080, a human fibrosarcoma cell line (JCRB9113; the Healthy Science Research Resources Bank), and its sublines were maintained at 37°C and 5% CO_2 in Dulbecco's modified Eagles medium (D-MEM) that was supplemented with 10% fetal bovine serum (FBS). The MIT-23 cell line was derived from HT1080 cells, in which Vpr expression is controlled by a tetracycline promoter, as described by Shimura *et al.* (1999b). For Vpr induction, 3 μg/ml DOX (Sigma, St Louis, MO, USA) was used. To obtain HT/DR-GFP, HT1080 cells were transfected with an inactive GFP expression cassette plasmid (pDR-GFP) and selected by puromycin (1 μg/ml), and clonal cell lines were established.

HIV infection

We used pseudotyped viruses that were defective for an envelope protein with *vpr* (R^+) or without *vpr* (R^-). HIV vectors were produced by transient transfection of 293T cells (Tokunaga *et al.*, 2001; Shimura *et al.*, 2005). The pNL-Luc-E^-R^+ or pNL-Luc-E^-R^- plasmid was co-transfected with pHIT/G using the transfection reagent Fugene-6 (Roche, Tokyo, Japan). Virus supernatants were collected at 48 h post-transfection. The harvested supernatants were centrifuged at 120 *g* for 5 min and stored at −80°C. Viral titers were measured by p24 ELISA (ZeptoMetrix). The virus was diluted in D-MEM supplemented with 10% FBS and used to infect HT1080 cells at a multiplicity of infection (MOI) of 0.8, which yielded about 80% of cells that were positive for luciferase expression (data not shown).

Protein analyses

The cells were washed with phosphate-buffered saline (PBS) and resuspended in radio-immunoprecipitation assay buffer composed of 50 mM Tris-HCl, 1% NP-40, 0.25%. sodium deoxycholate, 150 mM NaCl, 1 mM EGTA, 1 mM phenylmethysulfonyl fluoride, 1 μg/ml protease inhibitor mix, 1 mM Na_2VO_3 and 1 mM NaF. The cell suspension was sonicated. To fractionate chromatin fractions, cells were suspended in Buffer N (15 mM Tris-HCl (pH 7.5), 60 mM KCl, 15 mM NaCl, 5 mM $MgCl_2$, 1 mM $CaCl_2$, 1 mM DTT, 2 mM Na_2VO_3, 250 mM sucrose, protease inhibitors) with 0.6% NP-40. Cells were incubated on ice for 5 min followed by centrifugation (2000 *g*) to separate cytoplasmic proteins from nuclei. Isolated nuclei were then washed twice with Buffer N followed by resuspension in Lysis buffer (10 mM PIPES (pH 6.5), 10 mM EDTA, protease inhibitors) and centrifugation (6000 *g*) to extract soluble nuclear proteins. Finally, chromatin was resuspended in Lysis buffer and shared by sonication on ice to extract chromatin-bound proteins. The protein concentration was determined using the BCA protein assay reagent kit (Pierce). A 100-μg aliquot of protein from each cell extract was separated on 10% SDS–PAGE. Specific primary antibodies of p53 (Calbiochem), Chk2, ATM-S1981 (ATM-p), H2AX-S139 (γ-H2AX) and histone H3 (Upstate), Chk2-T68 (Chk2-p) and p53-S15 (p53-p) (Cell Signaling) were used for analysis. A monoclonal antibody to Vpr, 8D1 (IgG2a) was raised by immunization of a full-length Vpr peptide (Peptide Institute).

Immunoprecipitation was performed using 500 μg of protein mixed with 2 μg of anti-p53 protein-specific IgG-beads. Ternary complexes of protein A–antibody–antigen were collected by centrifugation and washed three times. The immunoprecipitates were subjected to SDS–PAGE followed by Western blot analysis. To obtain a rabbit antibody to RAD51, the human Rad51 protein was expressed as a recombinant protein in the *Escherichia coli* strain JM109 (DE3) (Kagawa *et al.*, 2001), and was purified as described previously (Kurumizaka *et al.*, 1999). Detection of target proteins was with an enhanced chemiluminescence detection system (Amersham Biosciences).

Immunostaining

The cells were washed with PBS and fixed with 2% paraformaldehyde in PBS and ice-cold methanol. The fixed cells were permeabilized with 0.2% Triton X-100 in PBS for 5 min. After treatment with PBS containing 10% goat serum for 30 min, the cells were incubated with primary antibodies that included rabbit polyclonal antibodies against Rad51 (1:400), mouse monoclonal antibodies against ATM-p (1:100) and γ-H2AX (1:100) (Upstate) and mouse monoclonal antibodies against BRCA1 (1:300) and RPA (1:1000) (Lab Vision). After 1 h of incubation at 37°C, secondary antibodies conjugated with Alexa 546 (1:1000; Molecular Probes, Eugene, OR, USA) were added for 1 h at 37°C. The slides were mounted in an anti-fade solution (KPL) and analysed by fluorescence microscopy.

Homologous recombination assay

The rate of extrachromosomal HR was assessed as previously described (Slebos and Taylor, 2001). HT1080 cells were co-transfected with pBHRF and pcDNA3.1/Vpr or pcDNA3.1 (Invitrogen). pBHRF encodes both a truncated GFP and full-length BFP. In the absence of HR, only BFP is expressed. However, HR between the BFP and truncated GFP results in the creation of a functional GFP. The green and blue fluorescence levels were examined simultaneously using a Vantage flow cytometer (Becton-Dickinson) equipped with a 488-argon laser (GFP) and a UV (350–360 nm) laser (BFP). *vpr* was derived from a NL4-3 clone (Adachi *et al.*, 1986). Each experiment was performed at least three times, and statistical analysis was carried out by Student's *t*-test.

The rate of intrachromosomal HR was assessed as reported in human glioma cells (Pierce *et al.*, 1999). Upon infection with Ad-I-Sce-I, a kind gift from Dr F Graham (McMaster University, Canada) or Ad-Lac8 (a gift from Dr I Saito, Tokyo University) as a control, GFP-positive cells as a result of HR were analysed. KU55933, a gift from Dr M O'Connor (KuDOS Pharmaceuticals, England), was dissolved in dimethylsulfoxide (DMSO). GFP was analysed with laser scanning cytometer

(LSC; Olympus, Tokyo, Japan) (Huang *et al.*, 2006). Cells cultured in cover slide were immersed in 0.2% Triton X-100 in PBS for 10 min. The slides were then incubated with anti-GFP antibody (1:100; Molecular Probes) before adding Alexa Fuor 488 conjugated secondary antibody (1:400; Molecular Probes). Green fluorescence emission was measured with LSC. The integrated fluorescence was measured in 10 000 cells for each sample. Each experiment was repeated three times, and statistical significance was examined.

Expression and purification of rVpr

rVpr was expressed in BL-21 codon plus (Stratagene) as a GST fusion protein and purified using glutathione column chromatography, as described (Hoshino *et al.*, submitted). Vpr eluted after precision treatment was applied to an affinity column coupled with a monoclonal antibody to Vpr, 8D1. After washing, Vpr was eluted with 100 mM Hepes buffer (pH 2.5), and immediately neutralized with 1 M Hepes buffer (pH 8.0). The concentration of rVpr was measured by an enzyme-linked immunosorbent assay version-1 by using two antibodies against Vpr, a monoclonal antibody (8D1), and a polyclonal antibody raised against a peptide of the carboxy-terminus of Vpr (IBL).

Acknowledgements

We are grateful to Dr T Takemori (National Institute of Infectious Diseases, Japan) to help for analysis by a Vantage flow cytometer. We also thank to Riken BRC for control adenovirus, AxCALac8, and HT1080 cells. Drs Slebos (National Institute of Environmental Health Science, USA), Jasin M (Memorial Sloan-Kettering Cancer Center, USA), Graham F (McMaster University, Canada), and Saito I (Institute of Medical Sciences, of Tokyo University, Japan) kindly provided us with pBHRF, pDR-GFP, adenovirus of I-*Sce*I, and AxCALac8, respectively. We also thank to O'Connor M (KuDOS pharmaceuticals, England) for KU55933. This work was supported by a Grant-in-Aid for Scientific Research from the Ministry of Health, Labor and a Grant for research on Health Sciences focusing on Drug Innovation. Dr Nakai-Murakami is a research resident supported by the Japan Health Sciences Foundation.

References

Abraham RT. (2001). *Genes Dev* **15**: 2177–2196.
Anglana M, Bacchetti S. (1999). *Nucleic Acids Res* **27**: 4276–4281.
Bartz SR, Rogel ME, Emerman M. (1996). *J Virol* **70**: 2324–2331.
Bertrand P, Saintigny Y, Lopez BS. (2004). *Trends Genet* **20**: 235–243.
Biggar RJ, Rosenberg PS, Coté T, Multistate AIDS/Cancer Match Study Group. (1996). *Int J Cancer* **68**: 754–758.
Brown EJ, Baltimore D. (2003). *Genes Dev* **17**: 615–628.
Bukrinsky M, Adzhubei A. (1999). *Rev Med Virol* **9**: 39–49.
Burgi A, Brodine S, Wegner S, Milazzo M, Wallace MR, Spooner K *et al.* (2005). *Cancer* **104**: 1505–1511.
Chadburn A, Cesarman E, Knowles DH. (1997). *Semin Diagn Pathol* **14**: 15–26.
Cromie GA, Connelly JC, Leach DRF. (2001). *Mol Cell* **8**: 1163–1174.
Daniel R, Greger JG, Katz RA, Taganov KD, Wu X, Kappes JC *et al.* (2004). *J Virol* **78**: 8573–8581.
Daniel R, Kao G, Tagarov K, Greger JG, Favorova O, Merkel G *et al.* (2003). *Proc Natl Acad Sci USA* **100**: 4778–4783.
Daniel R, Katz RA, Skalka AM. (1999). *Science* **284**: 644–647.
Daniel R, Marusich E, Argyris E, Zhao RY, Skalka AM, Pomerantz RJ. (2005). *J Virol* **79**: 2058–2065.
Dong Y, Hakimi MA, Chen X, Kumaraswamy E, Cooch NS, Godwin AK *et al.* (2003). *Mol Cell* **12**: 1087–1099.
Elder RT, Benko Z, Zhao Y. (2002). *Front Biosci* **7**: d349–d357.
Elenitoba-Johnson KS, Jaffe ES. (1997). *Semin Diagn Pathol* **14**: 35–47.
Goh WC, Rogel ME, Kinsey CM, Michael SF, Fultz PN, Nowak MA *et al.* (1998). *Nat Med* **4**: 65–71.
Groschel B, Bushman F. (2005). *J Virol* **79**: 5695–5704.
He J, Choe S, Walker R, Di Marzio PD, Morgan DO, Landau NR. (1995). *J Virol* **69**: 6705–6711.
Henklein P, Bruns K, Sherman MP, Tessmer U, Licha K, Kopp J *et al.* (2000). *J Biol Chem* **275**: 32016–32026.
Herida M, Mary-Krause M, Kaphan R, Cadranel J, Poizot-Martin IP, Rabaud C *et al.* (2003). *J Clin Oncol* **21**: 3447–3453.
Hoshino S, Sun B, Shimura M, Konishi M, Taguchi T, Segawa T *et al.* (2006). *submitted.*
Huang M-B, Weeks O, Zhao L-J, Saltarelli M, Bond VC. (2000). *J Neuro Viol* **6**: 202–220.
Huang X, Kurose A, Tanaka T, Traganos F, Dai W, Darzynkiewicz Z. (2006). *Cytometer A* **69A**: 222–229.
Ishizaka Y, Chernov MV, Burns CM, Stark GR. (1995). *Proc Natl Acad Sci USA* **92**: 3224–3228.
Yamaguchi-Iwai Y, Sonoda E, Buerstedde J-M, Bezzubova O, Morrison C, Takata M *et al.* (1998). *Mol Cell Biol* **18**: 6430–6435.
Jeanson L, Subra F, Vaganay S, Hervy M, Marangoni E, Bourhis J *et al.* (2002). *Virology* **300**: 100–108.
Jenkins Y, McEntee M, Weis K, Greene WC. (1998). *J Cell Biol* **143**: 875–885.
Kagawa W, Kurumizaka H, Ikawa S, Yokoyama S, Shibata T. (2001). *J Biol Chem* **276**: 35201–35208.
Khanna KK, Jackson SP. (2001). *Nat Genet* **27**: 247–254.
Khanna KK, Lavin MF, Jackson SP, Mulhern TD. (2001). *Cell Death Differ* **8**: 1052–1065.
Knowles DM. (2003). *Hematol Oncol Clin N Am* **17**: 785–820.
Kurumizaka H, Aihara H, Kagawa W, Shibata T, Yokoyama S. (1999). *J Mol Biol* **291**: 537–548.
Lai M, Zimmerman ES, Planelles V, Chen J. (2005). *J Virol* **79**: 15443–15451.
Lau A, Kanaar R, Jackson SP, O'Connor MJ. (2004). *EMBO J* **23**: 3421–3429.
Lau A, Swinbank KM, Ahmed PS, Taylor DL, Jackson SP, Smith GCM *et al.* (2005). *Nat Cell Biol* **7**: 493–500.
Laurence J, Astrin SM. (1991). *Proc Natl Acad Sci USA* **88**: 7635–7639.
Levy DN, Refaeli Y, MacGregor RR, Weiner DB. (1994). *Proc Natl Acad Sci USA* **91**: 10873–10877.
Li L, Olvera JM, Yoder KE, Mitchell RS, Butler SL, Lieber M *et al.* (2001). *EMBO J* **20**: 3272–3281.
Lim ST, Levine AM. (2005). *Curr HIV/AIDS Rep* **2**: 146–153.
Linke SP, Sengupta S, Khabie N, Jeffries BA, Buchhop S, Miska S *et al.* (2003). *Cancer Res* **63**: 2596–2605.
Mahalingam S, Ayyavoo V, Patel M, Kieber-Emmons T, Kao GD, Muschel RJ *et al.* (1998). *Proc Natl Acad Sci USA* **95**: 3419–3424.
Marmorstein LY, Ouchi T, Aaronson SA. (1998). *Proc Natl Acad Sci USA* **95**: 13869–13874.

Mayer V, Ebbesen P, Zachar V. (1995). *Eur J Cancer Prev* **4**: 211–212.
Nunnari G, Argyris E, Fang J, Mehlman KE, Pomerantz RJ, Daniel R. (2005). *Virology* **335**: 177–184.
O'Connell MJ, Walworth NC, Carr AM. (2000). *Trends Cell Biol* **10**: 296–303.
Pierce AJ, Johnson RD, Thompson LH, Jasin M. (1999). *Gene Dev* **13**: 2633–2638.
Roshal M, Kim B, Zhu Y, Nghiem P, Planelles V. (2003). *J Biol Chem* **278**: 25879–25886.
Sawaya BE, Khalili K, Mercer WE, Denisova L, Amini S. (1998). *J Biol Chem* **273**: 20052–20057.
Sengupta S, Linke SP, Pedeux R, Yang Q, Farnsworth J, Garfield SH *et al.* (2003). *EMBO J* **22**: 1210–1222.
Shiloh Y. (2001). *Curr Opin Genet Dev* **11**: 71–77.
Shimura M, Onozuka Y, Yamaguchi T, Hatake K, Takaku F, Ishizaka Y. (1999a). *Cancer Res* **59**: 2259–2264.
Shimura M, Tanaka Y, Nakamura S, Minemoto Y, Yamashita K, Hatake K *et al.* (1999b). *FASEB J* **13**: 621–637.
Shimura M, Tokunaga K, Konishi M, Sato Y, Kobayashi C, Sata T *et al.* (2005). *AIDS* **19**: 1434–1438.
Slebos RC, Taylor JA. (2001). *Biochem Biohpys Res Commun* **281**: 212–219.
Straus DJ. (2001). *Curr Oncol Rep* **3**: 260–265.
Tachiwana H, Shimura M, Nakai-Murakami C, Tokunaga K, Takizawa Y, Sata T *et al.* (2006). *Cancer Res* **66**: 627–631.
Taguchi T, Shimura M, Osawa Y, Suzuki Y, Mizoguchi I, Niino K *et al.* (2004). *Biochem Biophys Res Commun* **320**: 18–26.
Tokunaga K, Greenberg ML, Morse MA, Cumming RI, Lyerly HK, Cullen BR. (2001). *J Virol* **75**: 6776–6785.
van Gent DC, Hoeijmakers JHJ, Kanaar R. (2001). *Nat Rev Genet* **2**: 196–206.
Waldman AS, Liskay RM. (1987). *Proc Natl Acad Sci USA* **84**: 5340–5344.
West SC. (2003). *Nat Rev Mol Cell Biol* **4**: 1–11.
Yoon D, Wang Y, Stapleford K, Wiesmüller L, Chen J. (2004). *J Mol Biol* **336**: 639–654.
Yuan H, Kamata M, Xie Y-M, Chen ISY. (2004). *J Virol* **78**: 8183–8190.
Zhang H, Somasundaram K, Peng Y, Tian H, Zhang H, Bi D, Weber BL *et al.* (1998). *Oncogene* **16**: 1713–1721.
Zimmerman ES, Chen J, Andersen JL, Ardon O, DeHart JL, Blackett J *et al.* (2004). *Mol Cell Biol* **24**: 9286–9294.

Supplementary Information accompanies the paper on the Oncogene website (http://www.nature.com/onc).

Available online at www.sciencedirect.com
SCIENCE DIRECT®
Biochemical and Biophysical Research Communications 338 (2005) 1499–1506
BBRC
www.elsevier.com/locate/ybbrc

Improved gene expression in resting macrophages using an oligopeptide derived from Vpr of human immunodeficiency virus type-1

Izuru Mizoguchi [a,c], Yoshihiro Ooe [b], Shigeki Hoshino [a], Mari Shimura [a], Tadashi Kasahara [b], Shigeyuki Kano [a,c], Toshiko Ohta [c], Fumimaro Takaku [d], Yasuhide Nakayama [e], Yukihito Ishizaka [a,*]

[a] *Research Institute, International Medical Center of Japan, 1-21-1 Toyama, Shinjuku-ku, Tokyo 162-8655, Japan*
[b] *Biochemistry Department, Kyoritsu University of Pharmacy, 1-5-30 Shibakoen, Minato-ku 105-8512, Japan*
[c] *Institute of Basic Medical Sciences, University of Tsukuba, 1-1-1 Ten-nodai, Tsukuba 305-8577, Japan*
[d] *Jichi Medical School, 3311-1 Yakushiji, Minamikawachi-machi, Kawachi-gun, Tochigi 329-0498, Japan*
[e] *Department of Bioengineering, Advanced Medical Engineering Center, National Cardiovascular Center Research Institute, 5-7-1 Fujishiro-dai, Suita, Osaka 565-8565, Japan*

Received 13 October 2005
Available online 27 October 2005

Abstract

Vpr, an accessory gene product of human immunodeficiency virus type-1, is thought to transport a viral DNA from the cytoplasm to the nucleus in resting macrophages. Previously, we reported that a peptide encompassing amino acids 52–78 of Vpr (C45D18) promotes the nuclear trafficking of recombinant proteins that are conjugated with C45D18. Here, we present evidence that C45D18, when conjugated with a six-branched cationic polymer of poly(*N*,*N*-dimethylaminopropylacrylamide)-*block*-oligo(4-aminostyrene) (SV: star vector), facilitates gene expression in resting macrophages. Although there was no difference between SV alone and C45D18-SV with respect to gene transduction into growing cells, C45D18-SV resulted in more than 40-fold greater expression of the exogenous gene upon transduction into chemically differentiated macrophages and human quiescent monocyte-derived macrophages. The data suggest that C45D18 contributes to improving the ability of a non-viral vector to transduce macrophages with exogenous genes and we discuss its further application.

Keywords: HIV-1; Vpr; Nuclear trafficking; Star vector; Gene expression; Resting macrophages

Viral gene transfer systems are commonly used in current gene therapy protocols [1–3], but viral vectors can unfortunately cause side effects, such as severe immunological reactions [4] or leukemogenesis [5]. Thus, it is necessary to develop a non-viral vector system that is both safe and reliable. Various chemical compounds have been synthesized as non-viral vector candidates [6–9], but, in general, they need improvement to allow the expression of the exogenous genes in resting cells [9,10]. Among the obstacles to efficient gene transduction into resting cells is the nuclear membrane, which constitutes a critical barrier that impairs the efficient expression of exogenous genes [9,11]. Although there have been attempts to circumvent this problem, no reliable method has yet been established for effective transduction into resting cells [12–14].

The *vpr* gene, an auxiliary gene of human immunodeficiency virus type 1 (HIV) [15,16], encodes a virion-associated protein [17–19] and is a crucial factor in HIV-1 infection of resting macrophages [20]. It has been proposed that Vpr transports a pre-integration complex containing the viral DNA from the cytoplasm to the nucleus in infected cells [20]. Vpr has three α-helixes (amino acids 17–33, 38–50, and 56–77) [21] but no classical nuclear localization signals [22,23]. It is thought that the nuclear trafficking activity of

* Corresponding author.
E-mail address: zakay@ri.imcj.go.jp (Y. Ishizaka).

0006-291X/$ - see front matter © 2005 Elsevier Inc. All rights reserved.
doi:10.1016/j.bbrc.2005.10.112

Vpr is localized in the first and third α-helixes [24]. Interestingly, it has been postulated that Vpr transduces proteins as well as plasmid DNA into cells [25,26]. The activity is energy-independent and requires no cellular receptors [27]. A Vpr-derived peptide consisting of amino acids 52–96 has two biological properties that facilitate efficient gene expression: the arginine-rich stretch present in the carboxy (C)-terminal region, at amino acids 80–96, is required for the interaction with plasmid DNA and the third α-helix, at amino acids 52–70, enables trafficking of plasmid DNA through endosomes to the cytoplasm [28].

Recently, we identified a sequence corresponding to amino acids 52–78 (C45D18) as having protein transduction activity (Fig. 1A) [29]. When recombinant proteins are conjugated with C45D18 and added to the culture medium, they are quickly transported to the nucleus. This nuclear trafficking activity of C45D18 is also effective in resting cells, and C45D18-conjugated proteins were incorporated into most cells that were serum-starved during culture, as well as into peripheral blood mononuclear cells. This led us to hypothesize that C45D18 can be used to improve non-viral expression systems applicable to resting cells.

In this study, we combined C45D18 with a non-viral vector system, a cationic polymer named star vector (SV), which is a chemically synthesized gene transfer vector. SV is a nano-structured, hyperbranched, cationic star polymer with highly efficient transduction activity [30–33]. We found that C45D18-SV could induce efficient gene expression in both chemically differentiated macrophages and monocyte-derived macrophages (MDMs). We present the results of an analysis of the expression level of an exogenous gene and incorporated plasmid DNA. We also discuss the mechanism of the improved gene transduction using C45D18 and future applications of the peptide.

Materials and methods

Cell culture and chemicals. HeLa and HT1080 cells were cultured in Dulbecco's modified Eagle's medium (Invitrogen, Carlsbad, CA) supplemented with 10% fetal calf serum (FCS) (Sigma, St. Louis, MI). THP-1 cells (Riken Cell Bank, Tsukuba, Japan) were cultured in Iscove's modified Dulbecco's medium (IMDM) (Invitrogen) supplemented with 10% of FCS. To prepare resting cells, HT1080 cells were cultured for 3 days in 0.1% FCS medium. To differentiate THP-1, aliquots of 1×10^5 cells were plated onto each well of a poly-D-lysine-coated 6-well plate (Beckton–Dickinson, Benford, MA) and treated for 2 days with 5×10^{-8} M phorbol myristate acetate (PMA) (Sigma). The expression of Mac-1, a macrophage marker, was checked with a specific antibody (BD Pharmingen, San Diego, CA). To prepare human MDMs, peripheral blood mononuclear cells obtained from healthy humans were cultured for 4–7 days in the presence of 100 ng/ml of macrophage colony-stimulating factor (M-CSF) (R&D Systems, Minneapolis, MN) [34]. The expression of Mac-1, a macrophage marker, became positive after 2 days of culture (data not shown). For the transduction experiments, MDMs were cultured for an additional 4 days without M-CSF, and then the adherent cells were trypsinized and re-plated at a concentration of 2×10^5 cells per well in a 6-well plate.

Synthesis of hexakis(N,N-diethyldithiocarbamyl(oligo(4-aminostyrene)-block-poly(3-(N,N-dimethylamino)propylacrylamide)))methylbenzene (6-star-PDMAPAAm-b-OAS) (SV). Hexakis(bromomethyl)benzene and 4-aminostyrene (AS) (Sigma–Aldrich, Milwaukee, WI), sodium *N,N*-diethyldithiocarbamate (Wako Pure Chemical, Osaka, Japan), and 3-(*N,N*-dimethylamino)propylacrylamide (DMAPAAm) (Tokyo Kasei Kogyo, Tokyo, Japan) were purchased. Other chemical reagents were from Wako. A cationic star polymer with six poly[(*N,N*-dimethylamino)propylacrylamide] (PDMAPAAm) chains terminated with oligo(4-aminostyre) (OAS) per molecule (6-*star*-PDMAPAAm-*b*-OAS) was synthesized by iniferter-based photo-living radical polymerization of DMAPAAm and then AS from hexakis(*N,N*-diethyldithiocarbamylmethyl)benzene [32,33]. Briefly, hexakis(*N,N*-diethyldithiocarbamylmethyl)benzene was synthesized with reaction of hexakis(bromomethyl)benzene and sodium *N,N*-diethyldithiocarbamate, and crystallized from a chloroform–*n*-hexane solution. To synthesize 6-star-PDMAPAAm, the mixture of hexakis(*N,N*-diethyldithiocarbamylmethyl)benzene and DMAPAAm was irradiated for 30 min with a 200 W high pressure mercury lamp (Spot Cure, Ushio, Tokyo, Japan), concentrated, and dissolved in a small amount of methanol. The precipitate, obtained by the addition to ether (500 ml), was separated by filtration. Reprecipitation was performed in a methanol–ether system three times. The last precipitate was dried under vacuum to give 6-*star*-PDMAPAAm. To produce 6-star-PDMAPAAm-*b*-OAS, the mixture of 6-*star*-PDMAPAAm and AS was irradiated for 30 min under the above-mentioned conditions. The reaction mixture was concentrated and precipitated in 500 ml ether. Reprecipitation was carried out in a chloroform–ether system three times. The last precipitate was dried under vacuum to give 6-*star*-PDMAPAAm-*b*-OAS. The total molecular weight was about 18,300, which was estimated from GPC and ^{1}H NMR spectra. About 17.3 molecules of DMAPAAm unit and 1.4 molecules of AS unit were introduced to each terminal of all the six branch chains in the 6-*star*-PDMAPAAm-*b*-OAS.

Peptide synthesis and conjugation with SV. C45D18, other Vpr-derived peptides (shown in Fig. 1A), and Tat-derived peptide composed of GYGRKKRRQRRRGGC (single-letter amino acid code) [29] were synthesized chemically (Wako). Each peptide contains cysteine in C-terminal region and its SH-residue is used for conjugation to SV compound. Approximately 1 mg of SV was suspended in 1 ml of 10 mM phosphate buffer (pH 7.0) and added to 0.1 mM *N*-[*e*-maleimidocaproyloxy]succinimide ester (Dojindo Lab. Kumamoto, Japan). After 30 min at room temperature, each peptide was added and further incubated for 3 h at room temperature. The free peptides were removed by dialysis against phosphate-buffered saline overnight. The molar ratio of the peptide to SV was usually 3:1.

Cell cycle analysis. Cells were treated for 30 min, 1 or 2 days with 10 μM bromodeoxyuridine (BrdU) (Sigma). After fixation in 70% ice-cold ethanol, the cells were treated with an anti-BrdU antibody (Beckton–Dickinson) and then detected with Cy3-labelled antibody to mouse IgG (Molecular Probes, Eugene, OR).

Transfection and analysis of transduced genes. pLuc/EGFP constructed with pGL3 (Promega, Madison, WI) and pIRES2-EGFP (Clontech, Mountain View, CA) was used as a reporter construct. First, we examined complex formation involving the plasmid DNA and the peptides, SV and C45D18-SV. We incubated 250 ng of plasmid DNA with various amounts of peptides or other compounds in 150 μl Opti-MEM (Invitrogen). After 30 min at room temperature, the aliquots were loaded onto an agarose gel to determine the minimum amount of the compound required to completely neutralize the anionic charge of the DNA and then added to cell culture. After 48 h, luciferase assay was carried out (PicaGene, Toyoink, Tokyo, Japan). The protein concentration was measured by using a Bradford system (Bio-Rad, Hercules, CA) and the relative right units (RLUs) were normalized using the protein concentration.

To examine the level of exogenous gene expression, PCR analysis was carried out on reverse transcribed mRNA of the *GFP* gene. After transfection, mRNA was extracted using RNeasy (Invitrogen), and cDNA was synthesized with oligo(dT) (Qiagen, Hilden, Germany), and then amplified using an EX-Taq polymerase (TaKaRa, Shiga, Japan). To amplify the *β-actin* or *EGFP* genes, we used the respective forward and reverse primers 5′-TGAACCCCAAGGCCAACCGC-3′ and 5′-TTGTGCTGGGTGCCAGGGCA-3′ for *β-actin* or 5′-ATGGTGAGCAAGGGGCGA GGA-3′ and 5′-TTACTTGTACAGCTCGTCC-3′ (Hokkaido System Science, Sapporo, Japan) for *EGFP*. The amplified DNA was applied on an agarose gel, and the electrophoresed DNA was stained with Vistra Green

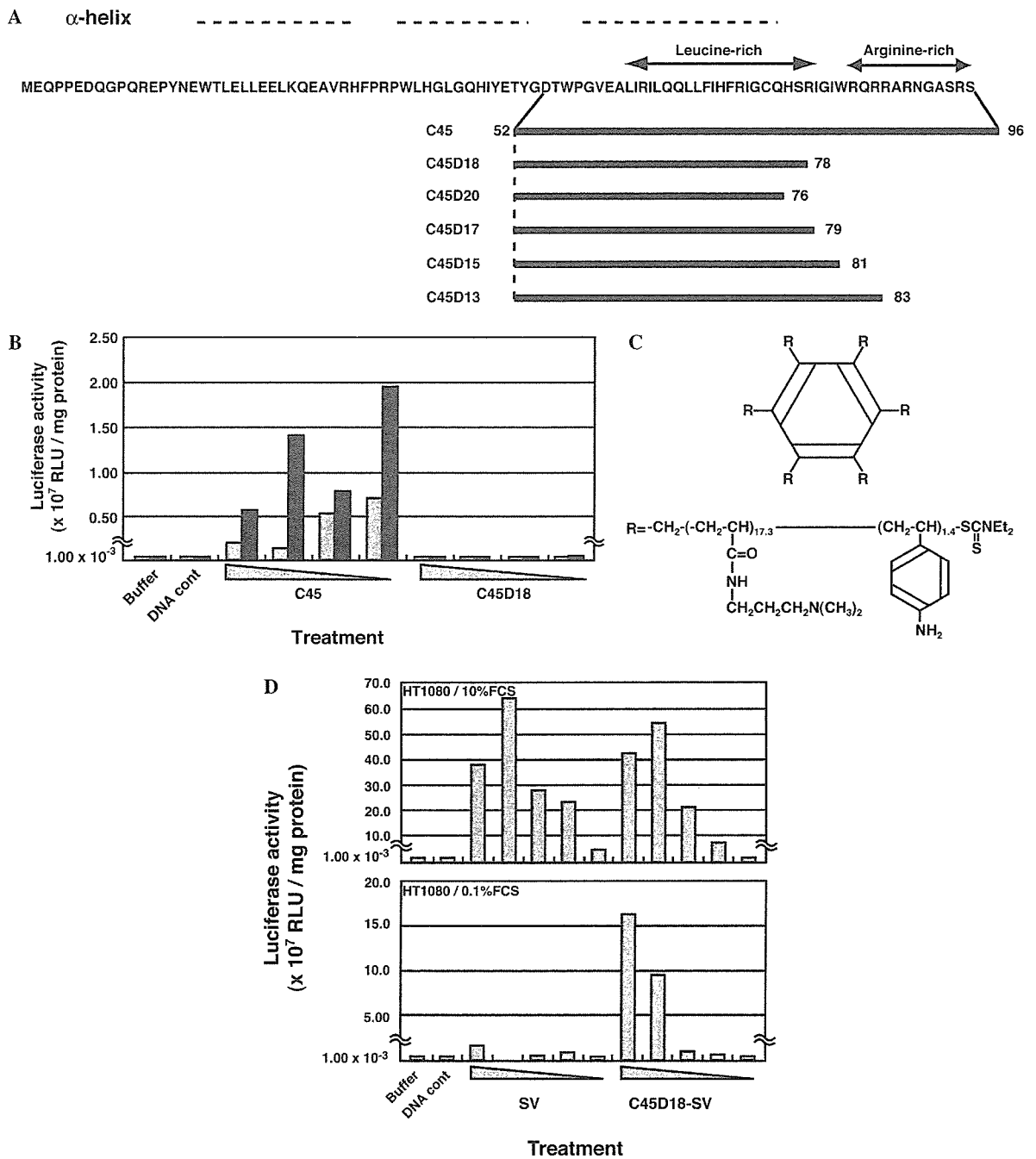

Fig. 1. Gene transduction by C45D18. (A) The amino acid sequences of the peptides used in this study. Amino acids are written using single-letter code. The α-helixes and arginine-rich stretch are also shown. Regions corresponding to six Vpr-derived peptides are depicted. (B) Gene transduction by C45 and C45D18 into growing cells. The reporter plasmid DNA, pLuc/EGFP, was mixed with C45 or C45D18, and was then added to HeLa (gray columns) or THP-1 (black columns) cells. Various concentrations of the peptides, ranging from 400 to 15 μM, were used. One representative result out of three independent experiments is shown. Luciferase activity is shown as relative light units (RLUs)/mg protein. (C) Schematic structure of SV. The SV used in this study has six branches (shown by "R") (21). The arrow indicates the amino residue that is used for conjugation with various peptides. (D) Efficient gene transduction by C45D18 into serum-starved cells. The gene transduction efficiencies using C45D18-SV and SV were compared. The HT1080 cells were cultured for 3 days in the presence of 0.1% FCS (lower panel) or under normal conditions (upper panel) and were then used for the experiments. The respective frequencies of BrdU-positive cells in the population were 9% and 43% for serum-starved cells and those cultured in the presence of 10% FCS, respectively. For each sample, 250 ng of plasmid DNA was mixed with 45–1.4 μM of the compounds.

(Amersham Biosciences, Piscataway, NJ). Then, the signal intensity of each band was measured using FX-PRO PLUS (Bio-Rad).

To analyze the plasmid DNAs incorporated in the nuclei, an aliquot of plasmid DNA was labeled with Cy3-dCTP (Amersham Biosciences), mixed with the same amount of plasmid DNA, and then used for transfection. The incorporated plasmid DNA was visualized using laser scanning microscopy (Bio-Rad). Cells positive for DNA aggregates that were larger than 2 μm were counted.

Statistical analysis. Statistical significance was evaluated using Student's *t* test.

Results

Gene transduction with C45 and C45D18

First, we compared the gene transduction activity of two peptides, C45 and C45D18 (Fig. 1A). Based on the results of a gel-shift assay to monitor the lipoplex formation of pLuc/EGFP (250 ng) with C45 (see Materials and methods), we used 15, 45, 135, and 400 μM of the peptide for the experiment. The C45 and an equivalent amount of C45D18 were incubated with plasmid DNA for 30 min at room temperature and were then added to cultures of HeLa and THP-1 cells. Consistent with previous reports [35,36], C45 was effective for gene transduction into these cells (Fig. 1B). By contrast, C45D18 did not show any transduction activity.

C45D18 facilitates gene transduction into resting cells

We previously reported that recombinant proteins, when conjugated with C45D18, could be transported into the nuclei of resting cells [29]. This finding led us to postulate that C45D18 could facilitate gene expression in resting cells, if an appropriate vehicle for the DNA were selected. To prove this, C45D18 was conjugated to SV (C45D18-SV; Fig. 1C), and we compared the efficiency of gene transduction using C45D18-SV with that using SV alone. Although the gene expression in growing cells was equivalent with both agents (Fig. 1D, upper panel), C45D18-SV resulted in more efficient gene expression in cells that had been cultured in the presence of 0.1% FCS (Fig. 1D, lower panel). Analysis of the cell cycle, judged using incorporated BrdU, revealed that the number of cells in S phase was decreased remarkably in the populations cultured in 0.1% FCS (9%) as compared with those cultured in 10% FCS (43%).

C45D18-SV increased the gene transfer to human macrophages

To obtain stronger evidence that C45D18 facilitates gene transduction into resting cells, we used THP-1 cells that had been treated with PMA. THP-1 is a non-adherent human monocytic leukemia cell line that acquires the macrophage-phenotype when cultured in the presence of PMA. Within 2 days after PMA treatment, THP-1 cells became adherent and positive for Mac-1, a macrophage-specific marker (data not shown). Then, we tested the efficacy of gene transduction using C45D18-SV. As shown in Fig. 2A, luciferase expression with C45D18-SV transduction was more than 40 times that with SV alone ($p < 0.05$). To examine the expression level of the exogenous gene, we amplified the *GFP* mRNA from transfectants treated with SV alone or with C45D18-SV and compared the intensities of the amplified DNA. As shown in Fig. 2B, the level of gene expression was increased strikingly in the cells treated with C45D18-SV (lane 2). Pulse-labeling with BrdU followed by detection with anti-BrdU

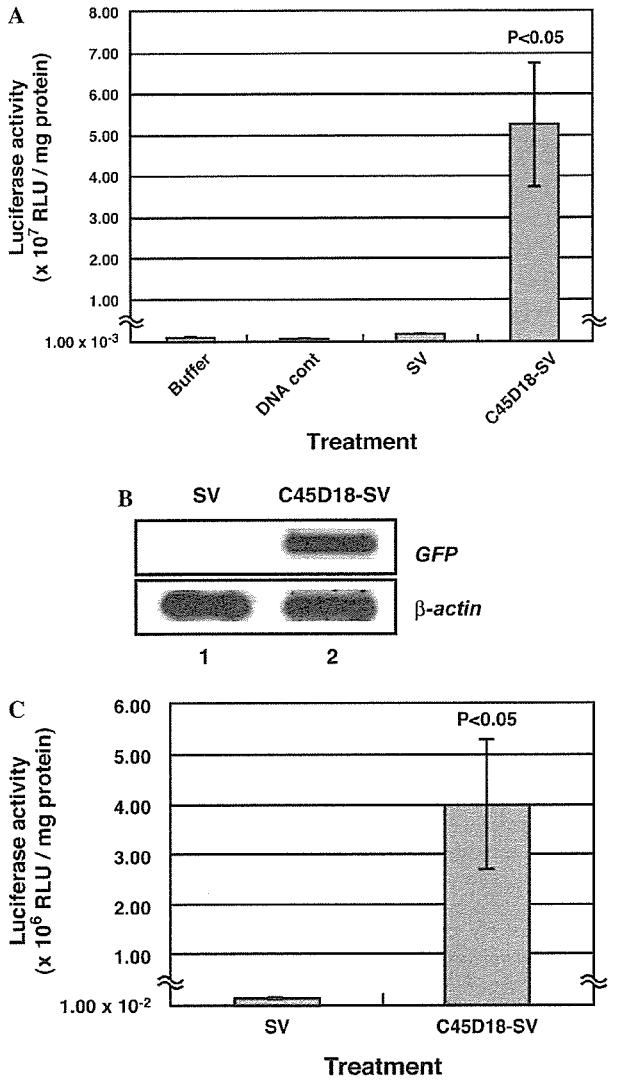

Fig. 2. Increased gene expression using C45D18-SV in resting macrophages. (A) The effects of C45D18-SV on chemically differentiated macrophages. THP-1 cells, after treatment for 2 days with PMA, were used for the transfection experiments. The experiments were carried out in triplicate, and the mean numbers and standard deviation were calculated. BrdU incorporation indicated that less than 1% of the cells were at S phase. Even with continuous exposure to BrdU for 2 days after transfection, less than 1% of the cells were BrdU-positive. (B) The expression of the exogenous gene using C45D18-SV in resting macrophages. RT-PCR analysis was performed using THP-1 cells treated with PMA and then transfected. As an internal control, β-actin mRNA was amplified. The results of the RT-PCR analysis of cells transduced using SV (lane 1) and C45D18-SV (lane 2) are shown. (C) Gene transduction into human macrophages. MDMs were prepared from healthy humans by culturing peripheral blood mononuclear cells for 6 days in the presence of 100 ng/ml M-CSF. Then, the cells were deprived of M-CSF for 4–5 days and subjected to experiments in triplicate. The mean value and standard deviation are shown, along with a representative result of three independent experiments. Immunohistochemical analyses of pulse-labeled BrdU and Mac-1 indicate that the prepared cells were resting macrophages (data not shown).

antibody revealed that less than 1% of PMA-treated THP-1 cells were positive for BrdU incorporation (data not shown), whereas about 30% of the untreated THP-1 cells were positive for BrdU incorporation. Moreover, with

continuous exposure to BrdU for 2 days after transfection, only 0.6% of the PMA-treated cells were labeled with BrdU (data not shown). These results indicate that THP-1 cells stop growing within 2 days after treatment with PMA and that C45D18-SV facilitates gene expression in resting macrophages.

Next, we focused on gene transduction into human MDMs using C45D18-SV. To test the efficacy of C45D18-SV, human macrophages were prepared by culturing peripheral blood mononuclear cells for 6 days in the presence of 100 ng/ml M-CSF. After cell expansion, the M-CSF was removed from the culture, and the culture was continued for another 4–5 days, which caused the expanded MDMs to stop growing (data not shown). Using these cells, we investigated the efficacy of C45D18. As shown in Fig. 2C, the transduction efficiency with C45D18-SV was significantly greater than that with SV alone ($p < 0.05$). We repeated the same experiments three times and obtained essentially the same statistically significant results.

C45D18-SV is the best molecule for gene transduction into macrophages

To determine the best Vpr-derived peptide for gene transfer into macrophages, several peptides were synthesized (Fig. 1A) and conjugated to SV at a molar ratio of 3:1. First, we compared the activities of C45 and C45D18. As shown in Table 1, C45-SV was much less potent than C45D18-SV in resting macrophages ($p < 0.01$), which is in contrast to the result, shown in Fig. 1B, that C45 induced much better gene expression in growing cells than did C45D18.

Next, we compared the activity of C45D18 with those of four other peptides. Based on several independent experiments, we estimated that the gene transduction efficiencies with C45D17, C45D15, C45D13, and C45D20 relative to that with C45D18 (1.0) were 0.25, 0.30, 0.45, and 0.32, respectively (Fig. 3A). Therefore, C45D18 is the minimum sequence giving the best efficiency of gene expression in resting macrophages.

Protein transduction activity has been well documented for Tat-derived peptide. Although the gene transduction activity of Tat has not been reported, we compared the gene transduction efficiency of Tat and C45D18. As shown in Fig. 3B, Tat-conjugated SV did not result in significant expression of the exogenous gene, whereas C45D18-SV reproducibly induced high expression from the plasmid DNA in resting macrophages.

Table 1
Gene-transducing activity of C45D18 and C45 to resting cells

Samples	RLU ($\times 10^{-5}$)/mg protein	Fold increase[b]	*t* test
Buffer	1.8 ± 0.4[a]	1	
DNA alone	2.7 ± 1.8	1.5	
SV alone	4.7 ± 2.0	2.7	
C45-SV	$11.4 \pm 6{,}4$	6.5	$p < 0.01$
C45D18-SV	96.6 ± 10.1	55.2	

[a] The relative right units (RLUs) were normalized using the protein concentration. The mean values and standard deviations were calculated from triplicate samples. Difference between luciferase activity obtained by C45-SV and C45D18-SV was statistically significant ($p < 0.01$).

[b] The fold increase was estimated using data for the buffer as control.

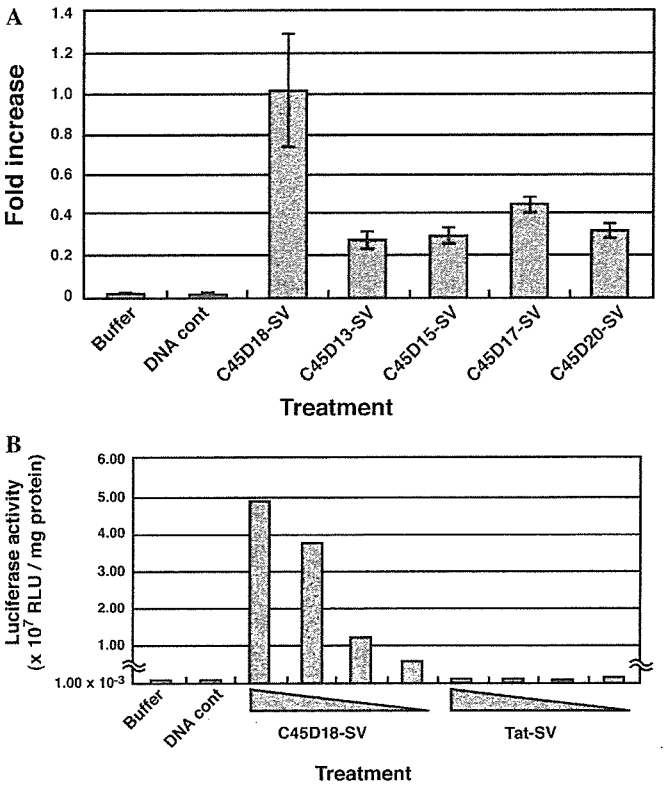

Fig. 3. C45D18 is the best molecule for efficient gene expression in resting macrophages. (A) Comparison of the gene transduction activities among C45D18 and four Vpr-derived peptides (see Fig. 1A). Each peptide was conjugated to SV at a molar ratio of 3:1, and the efficiency of gene expression in resting macrophages was analyzed. For each peptide, 17 μM peptide was reacted with 250 ng pLuc/EGFP. Three independent experiments were performed, and the mean and standard deviation were calculated. The activity of each peptide is given as a relative efficiency by defining the activity of C45D18-SV as 1.0. The actual luciferase activity obtained with C45D18-SV was $5.2 \pm 1.6 \times 10^7$ RLU/mg protein. (B) The effects of Tat-derived peptide on gene transfer into resting macrophages. Tat-derived peptide was conjugated to SV at a molar ratio of 3:1, and then the efficiency of gene expression in resting macrophages was examined. The maximum dose of each conjugated compound was 12 μM with 250 ng plasmid DNA. Each compound was serially diluted to 6, 3, and 1.5 μM, and the compound was reacted with the reporter plasmid DNA.

Condensed localization of exogenous DNA in the nucleus using C45D18-SV

To characterize the DNA incorporated in the nucleus by C45D18, we investigated the plasmid DNA in resting macrophages after transfection. For this purpose, an aliquot of plasmid DNA was labeled with Cy3-dCTP, mixed with an equal amount of unlabeled DNA, and used for the transfection experiment. Surprisingly, we observed the presence of plasmid DNA as large dots in the nucleus when C45D18-SV was used as the vector (Fig. 4A, right panels),

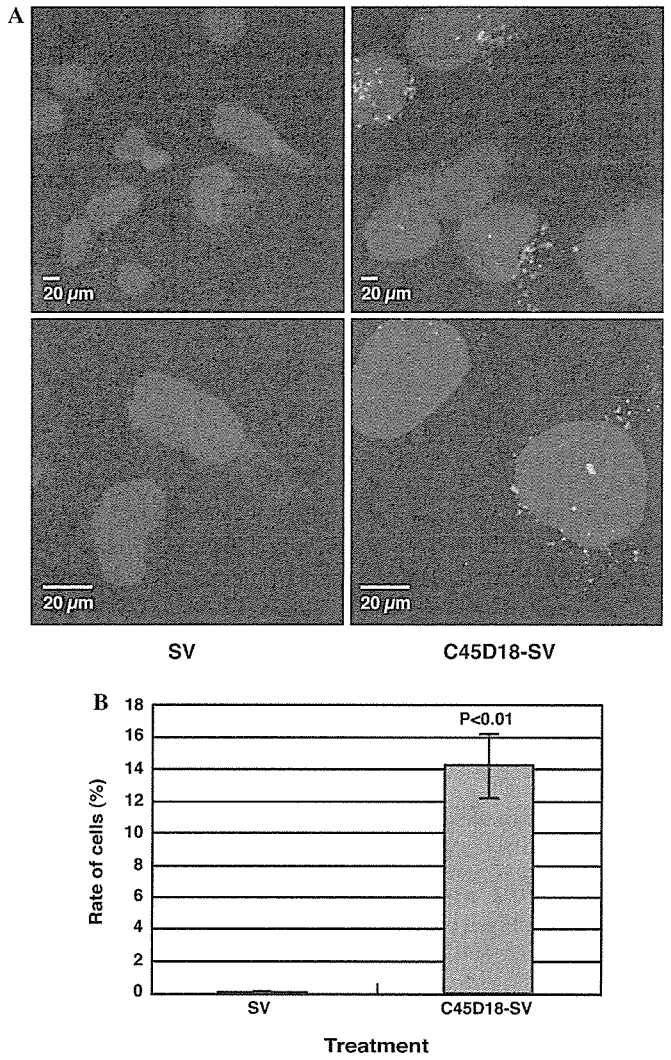

Fig. 4. Analysis of plasmid DNA introduced using C45D18-SV. (A) The aggregation of exogenous DNA in cells transduced with C45D18-SV. Plasmid DNA incorporated with SV (left panels) or C45D18-SV (right panels) was visualized using laser scanning microscopy. A small amount of plasmid DNA that had been pre-labeled with Cy3 was mixed with an equal amount of unlabeled plasmid DNA. The lower panels show enlarged cells. Plasmid DNA and nuclear DNA are shown in red and blue, respectively. The scale bar indicates 20 μm. (B) Increased number of cells with aggregated plasmid DNA. The number of cells containing large dots of plasmid DNA (>2 μm) was counted and plotted. At least 100 cells were counted per microscopic field. The mean and standard deviation were calculated using data obtained from three independent experiments. The difference between cells transduced using SV and those transduced using C45D18-SV was statistically significant ($p < 0.01$). (For interpretation of the references to color in this figure legend, the reader is referred to the web version of this paper.)

whereas fine dots of DNA were present in the cells transfected with SV alone (Fig. 4B, left panels). We counted the number of cells that contained labeled plasmid DNA dots larger than 2 μm. As shown in Fig. 4B, C45D18-SV dramatically increased the number of cells containing large dots of plasmid DNA; about 15% of the cells transduced with C45D18-SV contained large dots of aggregated plasmid DNA ($p < 0.01$). PCR analysis indicated that the copy number of plasmid DNA in cells treated with C45D18-SV was at most 1.7-fold that in cells treated with SV (data not shown).

Discussion

C45D18-SV is an effective, novel non-viral vector for gene transduction into human macrophages

We showed that C45D18 facilitates gene transduction into resting macrophages. In this work, we used SV as a vehicle for the plasmid DNA. SV is a synthetic cationic polymer used as a gene transfer vector [30]. It was previously demonstrated that SV can induce a gene transduction level 10-fold that induced with polyethyleneimine (PEI), which is one of the best agents popularly used for gene transfer [30]. Although SV by itself was not effective for introducing genes into chemically differentiated macrophages, C45D18-SV could promote the expression of exogenous genes at a significantly higher level (Figs. 2A and B). Furthermore, C45D18-SV could facilitate the expression of an exogenous gene in quiescent human MDMs (Fig. 2C). These results are consistent with our previous report that recombinant proteins conjugated with C45D18 could be transported into the nuclei of resting cells [29]. Based on these observations, we postulate that the C45D18-SV system will be effective for other types of resting cells. This possibility is now under investigation.

Of the peptides with protein transduction activity, it has been reported that Tat can transduce recombinant proteins, which are expressed as chimeric forms with Tat-derived peptide. In this work, we also tested the activity of the Tat-derived peptide, but Tat-SV induced few exogenous genes in resting macrophages (Fig. 3B). Therefore, C45D18 is the best candidate molecule for circumventing the difficulties of non-viral vector systems applied to resting cells.

Differential activity of C45D18 and C45

Interestingly, we observed a functional difference between C45 and C45D18. As reported [35,36], C45 could express plasmid DNA in growing cells (Fig. 1B), whereas C45D18 could not cause transduction alone; however, after conjugation to a cationic polymer, C45D18 showed unique activity, enabling gene expression in resting macrophages. By contrast, C45-SV was much less effective for gene transduction into resting cells (Table 1).

Vpr binds DNA through its C-terminal region [37]. C45D18 lacks the C-terminal region that is required for DNA binding, which explains why C45D18 alone could not cause gene expression. With C45D18 conjugated to SV, the cationic moiety of SV complemented the DNA binding property, restoring the nuclear trafficking activity of C45D18, which led to the transduction of genes into resting macrophages. By contrast, the conjugation of C45

to SV decreased its ability to cause gene expression in resting cells (Table 1). Both C45D18 and C45 were conjugated to SV through the cysteine residue at amino acid 76 of Vpr (see Materials and methods, and Fig. 1A). One possible explanation as to why C45 activity was decreased after conjugation to SV is that the interaction between the cationic moieties of C45 and SV interferes with the properties of the leucine/isoleucine-rich domain (LR-domain) of Vpr [23] (Fig. 1A). The LR-domain (amino acids 60–81) was reported to be required for nuclear trafficking of Vpr, and point mutations at amino acids 64, 67, 71, and 76 significantly reduced the Vpr activity of nuclear trafficking [24]. It would be important to conjugate C45D18 to other compounds through the third position of its C-terminal region to keep the amino half of C45D18 fully functional. In this context, it is likely that the nuclear trafficking activity of C45D18, if conjugated appropriately, would contribute to non-viral vector systems other than SV.

Effects of C45D18 on transduced plasmid DNA

Strikingly, the incorporated DNA aggregated in the nucleus when C45D18-SV was used as a transfer vector (Fig. 4A). About 15% of the cells were positive for large dots of plasmid DNA (>2 μm). By contrast, we detected few such cells after transduction by SV alone. It is still not known whether aggregated molecules are effective for gene expression. Although RT-PCR demonstrated that C45D18-SV strongly induced the expression of an exogenous gene (Fig. 2B), PCR analysis of the transduced DNA revealed that C45D18-SV did not dramatically increase the copy number of the exogenous gene, but gave at most 1.7 times the plasmid DNA produced with SV. These data suggest that C45D18-SV increased the local concentration of the plasmid DNA, resulting in increased expression of the exogenous gene.

The aggregation of plasmid DNA by C45D18 may impair the expression of the exogenous gene. When genes are transduced using a non-viral gene transfer system, the plasmid DNA must be released from the gene-transducing agent for efficient gene expression [38]. If the plasmid DNA transduced into nucleus is surrounded by the gene transfer agent, for example, by PEI, transcription cannot effectively occur [39]. When we examined the numbers of cells with exogenous gene expression, less than 1% of total cells were positive for GFP expression. Even in an immunohistochemical analysis with anti-GFP antibody, we observed that GFP-positive cells, indicating the transducing efficiency of the exogenous gene, increased to 0.5% from 0.1% on using C45D18-SV compared with SV alone. The data indicate that C45D18 increased the number of cells that are positive for expression of exogenous DNA, but most of the plasmid DNA transported into the nucleus unfortunately does not work well as a template for transcription. It is still necessary to develop a system in which exogenous genes transported to the nucleus by C45D18 are effectively released for favorable gene expression.

Acknowledgments

We thank Dr. Koetsu Ogasawara for offering advice regarding this study. This work was supported by a Grant-in-Aid for Scientific Research from the Ministry of Health, Labor and Welfare of Japan.

References

[1] G. Romano, P.P. Claudio, H.E. Kaiser, A. Giordano, Recent advances, prospects and problems in designing new strategies for oligonucleotide and gene delivery in therapy, In Vivo 12 (1998) 59–67.
[2] G. Romano, P. Michell, C. Pacilio, A. Giordano, Latest developments in gene transfer technology: achievements, perspectives, and controversies over therapeutic applications, Stem Cells 18 (2000) 19–39.
[3] K.K. Hunt, S.A. Vorburger, Tech. Sight. Gene therapy. Hurdles and hopes for cancer treatment, Science 297 (2002) 415–416.
[4] N. Boyce, In memoriam: tougher rules could be the legacy of gene therapy's first death, New Sci. 164 (1999) 9.
[5] J. Kaiser, Gene therapy. Seeking the cause of induced leukemias in X-SCID trial, Science 299 (2003) 495.
[6] H. Ma, S.L. Diamond, Nonviral gene therapy and its delivery systems, Curr. Pharm. Biotechnol. 2 (2001) 1–17.
[7] U. Lungwitz, M. Breunig, T. Blunk, A. Gopferich, Polyethylenimine-based non-viral gene delivery systems, Eur. J. Pharm. Biopharm. 60 (2005) 247–266.
[8] Y. Nagasaki, K. Yasugi, Y. Yamamoto, A. Harada, K. Kataoka, Sugar-installed block copolymer micelles, their preparation and specific interaction with lectin molecules, Biomacromolecules 2 (2001) 1067–1070.
[9] D.A. Dean, D.D. Strong, W.E. Zimmer, Nuclear entry of nonviral vectors, Gene Ther. 12 (2005) 881–890.
[10] A. Fasbender, J. Zabner, B.G. Zeiher, M.J. Welsh, A low rate of cell proliferation and reduced DNA uptake limit cationic lipid-mediated gene transfer to primary cultures of ciliated human airway epithelia, Gene Ther. 4 (1997) 1173–1180.
[11] F.M. Munkonge, D.A. Dean, E. Hillery, U. Griesenbach, E.W. Alton, Emerging significance of plasmid DNA nuclear import in gene therapy, Adv. Drug. Deliv. Rev. 55 (2003) 749–760.
[12] J. Zabner, A.J. Fasbender, T. Moninger, K.A. Poellinger, M.J. Welsh, Cellular and molecular barriers to gene transfer by a cationic lipid, J. Biol. Chem. 270 (1995) 18997–19007.
[13] T.K. Prasad, N.M. Rao, The role of plasmid constructs containing the SV40 DNA nuclear-targeting sequence in cationic lipid-mediated DNA delivery, Cell. Mol. Biol. Lett. 10 (2005) 203–215.
[14] S. Brunner, T. Sauer, S. Carotta, M. Cotten, M. Saltik, E. Wagner, Cell cycle dependence of gene transfer by lipoplex, polyplex and recombinant adenovirus, Gene Ther. 7 (2000) 401–407.
[15] F. Wong-Staal, P.K. Chanda, J. Ghrayeb, Human immunodeficiency virus: the eighth gene, AIDS Res. Hum. Retroviruses 3 (1987) 33–39.
[16] E.A. Cohen, R.A. Subbramanian, H.G. Gottlinger, Role of auxiliary proteins in retroviral morphogenesis, Curr. Top. Microbiol. Immunol. 214 (1996) 219–235.
[17] X.F. Yu, M. Matsuda, M. Essex, T.H. Lee, Open reading frame vpr of simian immunodeficiency virus encodes a virion-associated protein, J. Virol. 64 (1990) 5688–5693.
[18] W. Paxton, R.I. Connor, N.R. Landau, Incorporation of *vpr* into human immunodeficiency virus type 1 virions: requirement for the p6 region of *gag* and mutational analysis, J. Virol. 67 (1993) 7229–7237.
[19] E.A. Cohen, G. Dehni, J.G. Sodroski, W.A. Haseltine, Human immunodeficiency virus *vpr* product is a virion-associated regulatory protein, J. Virol. 64 (1990) 3097–3099.

[20] M.A. Vodicka, D.M. Koepp, P.A. Silver, M. Emerman, HIV-1 Vpr interacts with the nuclear transport pathway to promote macrophage infection, Genes Dev. 12 (1998) 175–185.
[21] N. Morellet, S. Bouaziz, P. Petitjean, B.P. Roques, NMR structure of the HIV-1 regulatory protein VPR, J. Mol. Biol. 327 (2003) 215–227.
[22] C. Dingwall, R.A. Laskey, Nuclear targeting sequences—a consensus? Trends Biochem. Sci. 16 (1991) 478–481.
[23] L.J. Zhao, S. Mukherjee, O. Narayan, Biochemical mechanism of HIV-I Vpr function. Specific interaction with a cellular protein, J. Biol. Chem. 269 (1994) 15577–15582.
[24] S. Mahalingam, V. Ayyavoo, M. Patel, T. Kieber-Emmons, D.B. Weiner, Nuclear import, virion incorporation, and cell cycle arrest/differentiation are mediated by distinct functional domains of human immunodeficiency virus type 1 Vpr, J. Virol. 71 (1997) 6339–6347.
[25] M.P. Sherman, U. Schubert, S.A. Williams, C.M. de Noronha, J.F. Kreisberg, P. Henklein, W.C. Greene, HIV-1 Vpr displays natural protein-transducing properties: implications for viral pathogenesis, Virology 302 (2002) 95–105.
[26] S.C. Piller, G.D. Ewart, A. Premkumar, G.B. Cox, P.W. Gage, Vpr protein of human immunodeficiency virus type 1 forms cation-selective channels in planar lipid bilayers, Proc. Natl. Acad. Sci. USA 93 (1996) 111–115.
[27] P. Henklein, K. Bruns, M.P. Sherman, U. Tessmer, K. Licha, J. Kopp, C.M. de Noronha, W.C. Greene, V. Wray, U. Schubert, Functional and structural characterization of synthetic HIV-1 Vpr that transduces cells, localizes to the nucleus, and induces G2 cell cycle arrest, J. Biol. Chem. 275 (2000) 32016–32026.
[28] Y. Jenkins, M. McEntee, K. Weis, W.C. Greene, Characterization of HIV-1 vpr nuclear import: analysis of signals and pathways, J. Cell Biol. 143 (1998) 875–885.
[29] T. Taguchi, M. Shimura, Y. Osawa, Y. Suzuki, I. Mizoguchi, K. Niino, F. Takaku, Y. Ishizaka, Nuclear trafficking of macromolecules by an oligopeptide derived from Vpr of human immunodeficiency virus type-1, Biochem. Biophys. Res. Commun. 320 (2004) 18–26.
[30] Y. Nakayama, T. Masuda, M. Nagaishi, M. Hayashi, M. Ohira, M. Harada-Shiba, High performance gene delivery polymeric vector: nano-structured cationic star polymers (Star vectors), Curr. Drug Deliv. 2 (2005) 53–57.
[31] Y. Nakayama, T. Matsuda, Surface macromolecular architectural designs using photo-graft copolymerization based on photochemistry of benzyl *N,N*-diethyldithiocarbamate, Macromolecules 29 (1996) 8622–8630.
[32] Y. Nakayama, M. Miyamura, Y. Hirano, K. Goto, T. Matsuda, Preparation of poly (ethylene glycol)-polystyrene block copolymers using photochemistry of dithiocarbamate as a reduced cell-adhesive coating material, Biomaterials 20 (1999) 963–970.
[33] Y. Nakayama, T. Matsuda, Surface macromolecular microarchitecture design: biocompatible surfaces via photo-block-graft-copolymerization using *N,N* diethyldithiocarbamate, Langmuir 15 (1999) 5560–5566.
[34] G. Li, Y.J. Kim, H.E. Broxmeyer, Macrophage colony-stimulating factor drives cord blood monocyte differentiation into IL-10(high)IL-12absent dendritic cells with tolerogenic potential, J. Immunol. 174 (2005) 4706–4717.
[35] A. Kichler, J.C. Pages, C. Leborgne, S. Druillennec, C. Lenoir, D. Coulaud, E. Delain, E. Le Cam, B.P. Roques, O. Danos, Efficient DNA transfection mediated by the C-terminal domain of human immunodeficiency virus type 1 viral protein R, J. Virol. 74 (2000) 5424–5431.
[36] E. Coeytaux, D. Coulaud, E. Le Cam, O. Danos, A. Kichler, The cationic amphipathic alpha-helix of HIV-1 viral protein R (Vpr) binds to nucleic acids, permeabilizes membranes, and efficiently transfects cells, J. Biol. Chem. 278 (2003) 18110–18116.
[37] S. Zhang, D. Pointer, G. Singer, Y. Feng, K. Park, L.J. Zhao, Direct binding to nucleic acids by Vpr of human immunodeficiency virus type 1, Gene 212 (1998) 157–166.
[38] M.B. Bally, P. Harvie, F.M. Wong, S. Kong, E.K. Wasan, D.L. Reimer, Biological barriers to cellular delivery of lipid-based DNA carriers, Adv. Drug. Deliv. Rev. 38 (1999) 291–315.
[39] V.K. Sharma, M. Thomas, A.M. Klibanov, Mechanistic studies on aggregation of polyethylenimine–DNA complexes and its prevention, Biotechnol. Bioeng. 90 (2005) 614–620.

Thermosensitive Properties of Poly(amidoamine) Dendrimers with Peripheral Phenylalanine Residues

Yohei Tono, Chie Kojima, Yasuhiro Haba, Toshinari Takahashi, Atsushi Harada, Shigeyuki Yagi, and Kenji Kono*

Department of Applied Chemistry, Graduate School of Engineering, Osaka Prefecture University, 1-1 Gakuen-cho, Sakai, Osaka 599-8531, Japan

Received January 7, 2006. In Final Form: March 29, 2006

Dendrimers are unique polymers with globular shapes and well-defined structures. We previously prepared poly(amidoamine) (PAMAM) dendrimers having phenylalanine (Phe) residues at every chain end of the dendrimer as efficient gene carriers. In this study, we found that Phe-derivatized PAMAM dendrimers change their water solubility depending on temperature. The dendrimers were soluble in aqueous solutions at low temperatures, but they became water-insoluble at temperatures above a specific threshold, which is termed the lower critical solution temperature (LCST). Although the LCST of Phe-modified dendrimers decreased with increasing dendrimer generation, these dendrimers exhibited an LCST of 20−30 °C under physiological conditions. In addition, the LCST of the dendrimers was controlled by introducing isoleucine (Ile) residues at chain ends of dendrimers at varying ratios with respect to Phe residues. The PAMAM dendrimers are known to encapsulate various drug molecules. For these reasons, temperature-sensitive dendrimers might be useful as efficient drug carriers with controlled size and temperature-responsive properties.

Many researchers in various fields, including drug and gene delivery, have applied dendrimers using advantages that conventional polymers do not have: globular shape and high controllability of chemical structure.[1] Although several dendrimers have been developed so far, poly(amidoamine)(PAMAM) dendrimers are studied most widely in biomedical fields.[2] PAMAM dendrimers have several features that are superior to those of other types of dendrimers. For example, their interior exhibits a high affinity for various molecules with negative charges, such as benzoic acid and methotrexate.[3] Their terminal functional groups, such as primary amine, hydroxyl, and carboxyl groups, are available for drug-molecule conjugation.[4] In addition, amine-terminated PAMAM dendrimers exhibit strong gene transfection activity to various types of cells in vitro and in vivo because of the so-called proton sponge effect that is induced by tertiary amines within the dendrimer.[5]

Recently, we prepared PAMAM G4 dendrimers with Phe residues at chain terminals to improve their transfection activity by synergy of the proton sponge effect and enhanced hydrophobic interaction.[6] Indeed, these Phe-modified dendrimers exhibited a high transfection activity with respect to animal cells, but we observed an unexpected and interesting property of the Phe-modified dendrimers. Here, we report temperature-sensitive properties of PAMAM dendrimers with Phe residues at their chain terminals.

Scheme 1. Preparation of PAMAM Dendrimers Having Various Amino Acid Residues[a]

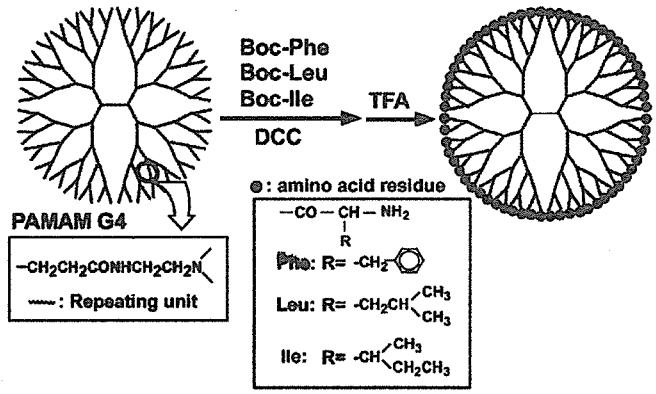

[a] DCC, *N,N'*-dicyclohexylcarbodiimide; TFA, trifluoroacetic acid.

PAMAM G3-G5 dendrimers with Phe residues were prepared by reacting amine-terminated PAMAM dendrimers with *tert*-butoxycarbonyl (Boc)-protected phenylalanine using condensing reagent *N,N'*-dicyclohexylcarbodiimide (DCC) and subsequent deprotection using trifluoroacetic acid (TFA), as reported previously (Scheme 1).[6] Using an identical method, PAMAM G4 dendrimers with leucine (Leu) or isoleucine (Ile) residues were prepared as dendrimers with hydrophobic amino acid residues of other types. The numbers of amino acid residues combined into PAMAM dendrimers were estimated from ^{1}H NMR spectra;[6] they are listed in Table 1. For all amino acid-derivatized dendrimers, the number of amino acid residues is consistent with the number of dendrimer chain ends, indicating that every chain end of a PAMAM dendrimer was combined with an amino acid residue.

Figure 1 shows transmittance at 600 nm for Phe-G4, Leu-G4, and Ile-G4 dendrimers dissolved in phosphate-buffered saline (PBS) of varying pH as a function of temperature. The Phe-G4 dendrimer solution was transparent below 28 °C but became

* Corresponding author. E-mail: kono@chem.osakafu-u.ac.jp. Tel: +81 72 254 9330. Fax: +81 72 254 9330.

(1) (a) Gillies, E.; Fréchet, J. M. J. *Drug Discovery Today* **2005**, *10*, 35. (b) Boas, U.; Heegaard, P. M. H. *Chem. Soc. Rev.* **2003**, *33*, 43. (c) Bosman, A. W.; Janssen H. M.; Meijer, E. W. *Chem. Rev.* **1999**, *99*, 1665. (d) Lee, C. C.; MacKay, J. A.; Fréchet, J. M. J.; Szoka, F. C. *Nat. Biotech.* **2005**, *23*, 1517.

(2) (a) Roberts, J. C.; Bhalgat, M. K.; Zera, R. T. *J. Biomed. Mater. Res.* **1996**, *30*, 53. (b) Patri, A. K.; Majoros, I. J.; Baker, J. R., Jr. *Curr. Opin. Chem. Biol.* **2002**, *6*, 466. (c) Stenson, S.; Tomalia, D. A. *Adv. Drug Delivery Rev.* **2005**, *57*, 2106.

(3) (a) Kojima, C.; Kono, K.; Maruyama K.; Takagishi, T. *Bioconjugate Chem.* **2000**, *33*, 9169. (b) Kojima, C.; Haba, Y.; Fukui, T.; Kono, K.; Takagishi, T. *Macromolecules* **2003**, *36*, 2183. (c) Beezer, A. E.; King, A. S.; Martin, I. K.; Mitchel, J. C.; Twyman, L. J. Wain, C. F. *Tetrahedron* **2003**, *59*, 3873.

(4) (a) Quintana, A.; Raczka, E.; Piehler, L.; Lee, I.; Myc, A.; Majoros, I.; Patri, A. K.; Thomas, T.; Mule, J.; Baker, J. R., Jr. *Pharm. Res.* **2002**, *19*, 1310. (b) Malik, N.; Evagoras; E.; Duncan, R. *Anti-Cancer Drugs* **1999**, *10*, 767. (c) Khandare, J.; Kolhe, P.; Pillai, O.; Kannan, S.; Lieh-Lai, M.; Kannan, R. M. *Bioconjugate Chem.* **2005**, *16*, 330.

(5) (a) Haensler, J.; Szoka, F. C., Jr. *Bioconjugate Chem.* **1993**, *4*, 372. (b) Kukowska-Latallo, J. F.; Bielinska, A. U.; Johnson, J.; Spindler, R.; Tomalia, D. A.; Baker, J. R., Jr. *Proc. Natl. Acad. Sci. U.S.A.* **1996**, *93*, 4897. (c) Takahashi, T.; Harada, A.; Emi, N.; Kono, K. *Bioconjugate Chem.* **2005**, *16*, 1160.

(6) Kono, K.; Akiyama, H.; Takahashi, T.; Takagishi, T.; Harada, A. *Bioconjugate Chem.* **2005**, *16*, 208.

10.1021/la060066t CCC: $33.50
Published on Web 04/22/2006

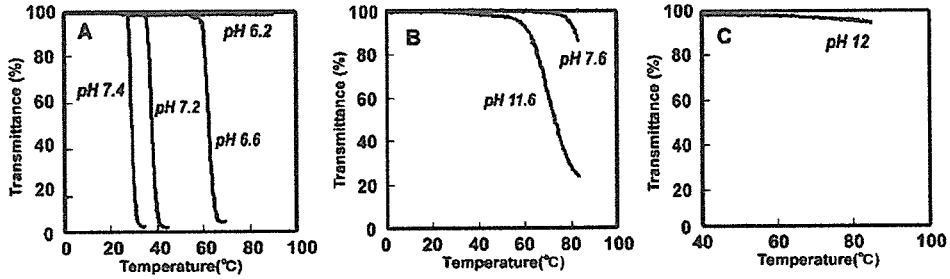

Figure 1. Transmittance of Phe-G4 (A), Leu-G4 (B), and Ile-G4 (C) dendrimers dissolved in PBS of varying pH. The dendrimer concentration was 1.0 mg/mL.

Table 1. Number of Amino Acid Residues Attached to a Dendrimer[a]

dendrimer	number of chain ends	number of amino acid residues
Phe-G3	32	31.8
Phe-G4	64	63.8
Leu-G4	64	64.3
Ile-G4	64	63.8
Phe-G5	128	129.1

[a] Estimated by ^{1}H NMR.

very turbid, indicating that this dendrimer exhibits an LCST. The LCST of the Phe-G4 dendrimer was dependent on the solution pH: its LCST increased with decreasing pH. Protonation of tertiary amines in the PAMAM dendrimer interior occurs below pH 7.0.[7] Therefore, the increase in the LCST is probably attributable to their protonation below that pH level. In fact, we have observed that the LCST of PAMAM dendrimers with isobutyramide groups at chain terminals, which were another type of thermosensitive dendrimer, increased at pH lower than 7.0.[8] For the Phe-modified dendrimer, protonation of the tertiary amine groups in the interior might be suppressed because derivatization with the bulky amino acid residues renders the dendrimer more globular. For that reason, its interior would be more crowded, as identified by comparison between low-energy conformers of the Phe-G4 dendrimer and its parent dendrimer obtained using Chem 3D software (Supporting Information). Nevertheless, the Phe-G4 dendrimer showed an LCST pH dependence above pH 7.0. Consequently, it is likely that the protonation of both α-amino groups of Phe residues and interior tertiary amines contributed to the pH dependence of the dendrimer LCST.

Figure 1B shows that the water solubility of the Leu-G4 dendrimer decreased above 60 °C. However, compared to the case of the Phe-G4 dendrimer, the solubility change in the Leu-G4 dendrimer was less pronounced; it occurred only at high pH. In addition, the water solubility of the Ile-G4 dendrimer (Figure 1C) did not change under these experimental conditions. The appearance of the LCST is inferred to be related to the balance between the hydrophobicity and hydrophilicity of the molecule. The LCST of thermosensitive polymers is known to increase with increasing hydrophilicity. For example, Ito reported that the LCST of poly(*N*-alkylacrylamide)s increases with increasing alkyl chain length of the side groups.[9] The partition coefficient (K_{ow}) between *n*-octanol and water is widely used to estimate molecular hydrophilicity and hydrophobicity. The $\log_{10} K_{ow}$ values for phenylalanine, leucine, and isoleucine were reported re-

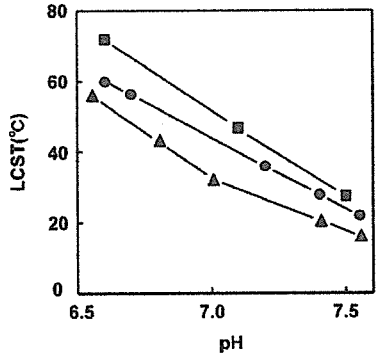

Figure 2. LCST of Phe-G3 (■), Phe-G4 (●), and Phe-G5 (▲) dendrimers dissolved in PBS as a function of pH. The dendrimer concentration was 1.0 mg/mL.

spectively as −1.35, −1.52, and −1.69,[10] indicating that Leu and Ile residues are less hydrophobic than the Phe residue. It is probable that the Phe residues provide the proper hydrophobicity–hydrophilicity balance to the dendrimer for the appearance of the LCST, whereas Leu and Ile residues might be too hydrophilic to yield a dendrimer with a thermosensitive property around neutral pH.

We next investigated the influence of dendrimer generation on the LCST. Figure 2 shows that the dendrimer with a higher generation exhibited a lower LCST at the same pH. Interaction between Phe residues is likely to be crucial to the appearance of the dendrimers' thermosensitive properties. Therefore, we tried to estimate the surface density of Phe residues for these Phe-modified dendrimers using molecular modeling. The minimum-energy conformers for the Phe-modified and unmodified dendrimers were obtained using Chem3D software (Supporting Information). Although a quantitative estimation of the surface density of Phe residues is difficult, the Phe density seems to increase with dendrimer generation. The diameters of PAMAM G3, G4, and G5 dendrimers are reported to be 3.6, 4.5, and 5.4 nm.[11] Consequently, the Phe residues' densities are calculated to be 0.8, 1.0, and 1.4 Phe residues/nm^2, respectively, for Phe-G3, Phe-G4, and Phe-G5 dendrimers by assuming that the dendrimers have spherical, rigid geometry. Of course, their actual topology might be oversimplified by this assumption.

It is generally considered that the interaction among hydrophobic side chains plays an important role in the occurrence of temperature-induced conformational transitions and changes in the water solubility of thermosensitive polymers.[7,12] Dense packing of Phe residues in the dendrimer periphery would enhance the interaction among side groups of Phe residues. In addition,

(7) (a) Niu, Y.; Sun, L.; Crooks, R. M. *Macromolecules* **2003**, *36*, 5725. (b) Cahara, D.; Kleimann, J.; Borkovec, M. *Macromolecules* **2003**, *36*, 4201.
(8) Haba, Y.; Harada, A.; Takagishi, T.; Kono, K. *J. Am. Chem. Soc.* **2004**, *126*, 12760.
(9) Ito, S. *Kobunshi Ronbunshu* **1989**, *46*, 437.
(10) Klein, R. A.; Moore, M. J.; Smith, M. W. *Biochim. Biophys. Acta* **1971**, *233*, 420.
(11) Tomalia, D. A.; Naylor, A. M.; Goddard, W. A., III *Angew. Chem., Int. Ed. Engl.* **1990**, *29*, 138.
(12) (a) Shild, H. G. *Prog. Polym. Sci.* **1992**, *17*, 163. (b) Suwa, K.; Morishita, K.; Kishida, A.; Akashi, M. *J. Polym. Sci., Part A: Polym. Chem.* **1997**, *35*, 3087.

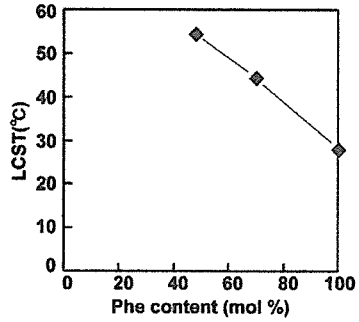

Figure 3. LCST of PAMAM G4 dendrimers having Phe and Ile residues as a function of the content of Phe residues (mol %) in the peripheral amino acid residues. LCST was measured with dendrimers dissolved in PBS (1.0 mg of dendrimer/mL, pH 7.4).

an increase in the Phe residues' density on the dendrimer surface should serve to elevate the dendrimer's hydrophobicity. Topological changes are known to take place in dendrimer molecules as a function of their generation number. The G3 dendrimer is reported to be highly asymmetric, whereas the G5 dendrimer is nearly spherical, with the transition between two forms occurring at the G4 dendrimer.[13] Derivatization occurring by attaching the bulky amino acid Phe to the chain termini might induce more spherical dendrimer topology. For that reason, Phe-modified dendrimers with a higher generation number might exhibit a lower LCST. A similar generation dependence of the LCST was observed for isobutyramide-terminated PAMAM or polypropylenimine dendrimers.[8]

Finally, we examined the control of the dendrimer LCST. The LCST for conventional thermosensitive polymers with a linear structure was controlled by copolymerization with comonomers with appropriate hydrophilicity or hydrophobicity.[14] We applied that strategy to control the LCST of thermosensitive Phe-modified dendrimers and used Ile as a hydrophilic unit. We reacted the amine-terminated PAMAM G4 dendrimer with mixtures of Boc-Phe and Boc-Ile, respectively, in ratios of 3/7 and 5/5 (mol/mol) and thereby prepared two kinds of PAMAM G4 dendrimers that have Phe and Ile residues: a dendrimer with 30 Phe and 34 Ile residues and a dendrimer having 44 Phe and 20 Ile residues per dendrimer molecule. Phenylalanine was more readily incorporated into the dendrimer because the Phe residues attached to the dendrimer might enhance the association of phenylalanine to the dendrimer through their interaction in the dendrimer periphery.[15]

Figure 3 shows the relationship between the dendrimer LCST and the percentage of Phe residues in the surface amino acid residues. The LCST of the dendrimer decreased as the Phe content in the dendrimer surface increased. This result indicates that the LCST of the dendrimer may be controlled by the ratio of Phe and Ile residues at the chain terminals. It is noteworthy that the dendrimer having 44 Phe and 20 Ile residues exhibited an LCST at 45 °C because dendrimers that express a temperature response a few degrees above physiological temperature might be useful for target-specific drug delivery in combination with local hyperthermia.[16]

In conclusion, we demonstrated that the incorporation of phenylalanine into chain terminals of PAMAM dendrimers endows them with temperature-sensitive water solubility. In addition, the temperature at which the dendrimers exhibited a temperature response can be controlled by the introduction of more hydrophilic amino acid residues such as Ile. Other than the Phe-modified PAMAM dendrimers, only a few types of dendrimers have been reported to exhibit LCSTs.[8,17] Among these temperature-sensitive dendrimers, those prepared in this study might be more suitable for use in biomedical fields because they have a surface of naturally occurring amino acid residues. In addition, these dendrimers were shown to change the LCST dependence on pH. Considering their application to drug and gene delivery, this property is of interest because when taken up by a cell through endocytosis these dendrimers might change their properties in endosomes/lysosomes, which have an acidic interior. Both temperature-sensitive and pH-sensitive dendrimer properties might be useful for controlling interactions with the target site and for controlling the retention and release of bioactive molecules.

Supporting Information Available: Synthesis and characterization of dendrimers, ^{1}H NMR spectra of Phe-Leu G4 dendrimers, analytical techniques, and low-energy conformers of dendrimers obtained using Chem3D software. This material is available free of charge via the Internet at http://pubs.acs.org.

LA060066T

(13) Naylor, A. M.; Goddard, W. A., III; Kiefer, G. E.; Tomalia, D. A. *J. Am. Chem. Soc.* **1989**, *111*, 2339.

(14) (a) Chen, G.; Hoffman, A. S. *Nature* **1995**, *373*, 49. (b) Feil, H.; Bae, Y. H.; Feijen, J.; Kim, S. W. *Macromolecules* **1993**, *26*, 2496. (c) Hayashi, H.; Kono, K.; Takagishi, T. *Bioconjugate Chem.* **1999**, *10*, 412.

(15) Jansen, J. F. G. A.; de Brabander-van den Berg, E. M. M.; Meijer, E. W. *Science* **1994**, *266*, 1226.

(16) Weinstein, J. N.; Magin, R. L.; Yatvin, M. B.; Zaharko, D. S. *Science* **1979**, *204*, 188.

(17) Parrott, M. C.; Marchington, E. B.; Valliant, J. F.; Adronov, A. *J. Am. Chem. Soc.* **2005**, *127*, 12081.

Temperature Sensitization of Liposomes by Use of *N*-Isopropylacrylamide Copolymers with Varying Transition Endotherms

Keisuke Yoshino, Atsushi Kadowaki, Toru Takagishi, and Kenji Kono*

Department of Applied Materials Science, Graduate School of Engineering, Osaka Prefecture University, 1-1, Gakuen-cho, Sakai, Osaka 599-8531, Japan. Received November 6, 2003; Revised Manuscript Received May 28, 2004

Three kinds of copolymers of *N*-isopropylacrylamide (NIPAM) with the same conformational transition temperature and varying transition endotherms were synthesized with *N*-acryloylpyrrolidine (APr), *N*,*N*-dimethylacrylamide (DMAM), and *N*-isopropylmethacrylamide (NIPMAM) as the comonomers. Two dodecyl groups were incorporated into the termini of these copolymers as an anchor for the fixation to a liposomal membrane. Egg yolk phosphatidylcholine liposomes having these copolymers were prepared and their temperature-sensitive contents release and association properties were investigated. While these copolymer exhibited a conformational transition at ca. 40 °C, ΔH for the transition increased in the order of poly(APr-*co*-NIPAM) < poly(DMAM-*co*-NIPAM) < poly(NIPMAM-*co*-NIPAM). The liposomes containing poly(NIPMAM-*co*-NIPAM) showed a drastic release enhancement of entrapped calcein above the transition temperature, whereas the liposomes with poly(DMAM-*co*-NIPAM) and those with poly(APr-*co*-NIPAM) exhibited moderate and slight enhancement of calcein release above that temperature, respectively. On the contrary, the liposomes containing poly(APr-*co*-NIPAM) showed significant aggregation above the transition temperature, but the aggregation was hardly observed for the liposomes having poly(NIPMAM-*co*-NIPAM), indicating that poly(APr-*co*-NIPAM) more efficiently made the liposome surface hydrophobic. Thus, we concluded that the copolymer with a large ΔH is suitable for obtaining functional liposomes with a temperature-sensitive contents release property, whereas the copolymer with a small ΔH is appropriate for preparing functional liposomes with a temperature-sensitive surface property.

1. INTRODUCTION

Liposomes have been considered to be a highly attractive material as drug carriers, because of their merits, such as biocompatibility, ability to encapsulate both hydrophilic and hydrophobic drugs, and size controllability (*1*). To increase their usefulness as drug carriers, many efforts have been made to provide liposomes with various functions. pH-Sensitive (*2*−*4*), light-sensitive (*5*−*8*), and temperature-sensitive (*9*−*11*) liposomes have been extensively studied as functional liposomes, which are useful for site-specific and/or cytoplasmic drug delivery.

While several approaches have been employed for the production of functional liposomes, modification of the liposomes with functional polymers is one of the most effective methods (*12*−*14*). For example, Tirrell and coworkers (*3*, *13*) have achieved the sensitization of egg yolk phosphatidylcholine (EYPC) liposomes to pH by the conjugation of a pH-sensitive polymer, poly(2-ethylacrylic acid), which strongly binds to lipid membranes and permeabilizes them. In addition, various synthetic polymers and peptides containing carboxyl groups have been used to render stable liposomes pH-sensitive (*15*−*17*).

Recently, the temperature sensitization of liposomes has been actively attempted by use of thermosensitive polymers, such as poly(*N*-isopropylacrylamide) [poly(NIPAM)] (*14*, *18*−*21*). Poly(NIPAM) is known to exhibit a lower critical solution temperature (LCST) at ca. 32 °C (*22*). This polymer is hydrophilic and soluble in water below the LCST. However, it becomes hydrophobic and forms an insoluble aggregate above this temperature due to hydrophobic interactions and hydrogen bonding. At the molecular level, it undergoes a coil-to-globule transition at the LCST. We have shown that when a homopolymer and copolymers of NIPAM are fixed onto the liposome surface, contents release from the liposome can be triggered by increasing the temperature above their LCST (*18*, *20*, *23*). In addition, it has been demonstrated that surface modification with these thermosensitive polymers provides liposomes with temperature-sensitive surface properties. For example, the hydrophobicity and surface charge density of the thermosensitive polymer-modified liposomes were shown to be controlled by the ambient temperature (*24*, *25*).

The functions of the thermosensitive polymer-modified liposomes are generated through the interaction between the fixed thermosensitive polymer and the liposome membrane. Their performance should be affected by the mechanism and strength of their interaction. The ability of thermosensitive polymers to sensitize liposome membranes should depend on their structures and characteristics. Therefore, for the development of functional liposomes with high temperature sensitivity, it is important to know what characteristics of the thermosensitive polymers will affect their ability to sensitize liposomes.

In this study, three kinds of NIPAM copolymers, which undergo a conformational transition at the same temperature but exhibit different transition endotherms, were synthesized with *N*-acryloylpyrrolidine (APr), *N*,*N*-

* Corresponding author: Tel +81-72-254-9330; fax +81-72-254-9913; e-mail kono@ams.osakafu-u.ac.jp.

10.1021/bc034205j CCC: $27.50
Published on Web 08/21/2004

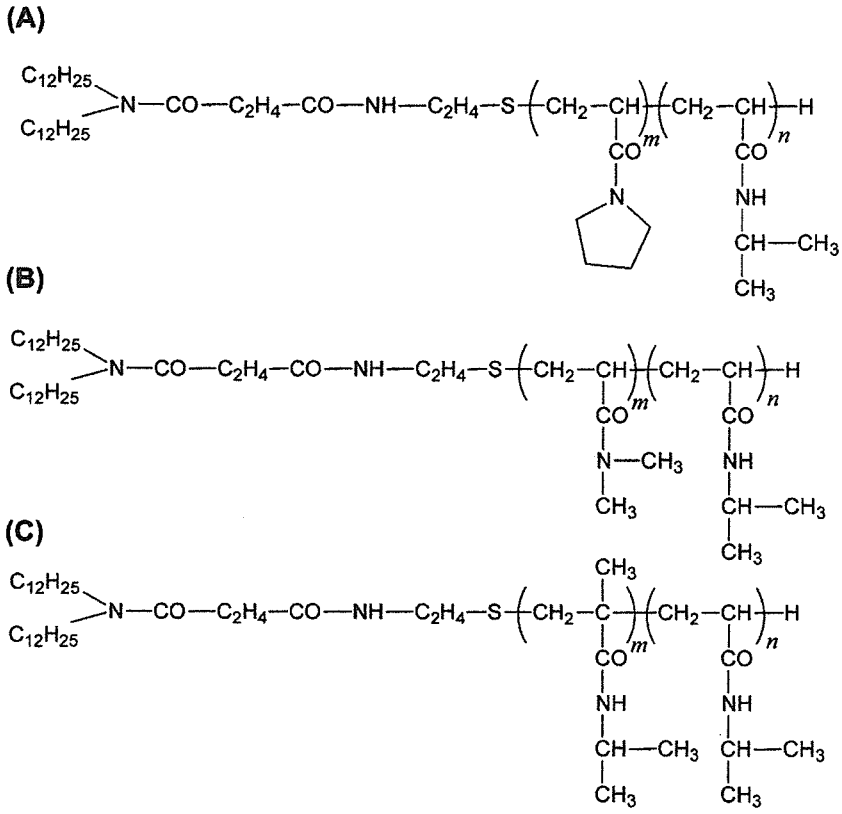

Figure 1. Structures of $2C_{12}$-poly(APr-*co*-NIPAM) (A), $2C_{12}$-poly(DMAM-*co*-NIPAM) (B), and $2C_{12}$-poly(NIPMAM-*co*-NIPAM) (C).

dimethylacrylamide (DMAM), and *N*-isopropylmethacrylamide (NIPMAM) as comonomers. Two dodecyl groups were connected to the chain end of these copolymers as an anchor to a liposomal membrane. These anchor-bearing copolymers are termed $2C_{12}$-poly(APr-*co*-NIPAM), $2C_{12}$-poly(DMAM-*co*-NIPAM), and $2C_{12}$-poly(NIPMAM-*co*-NIPAM) (Figure 1). The close correlation between the transition enthalpies of the copolymers and their ability to sensitize liposomes has been described.

2. EXPERIMENTAL SECTION

2.1. Materials. EYPC was kindly donated by Nippon Oil and Fats Co. (Tokyo, Japan). NIPAM, 2-aminoethanethiol, and Triton X-100 were supplied from Tokyo Kasei (Tokyo, Japan). Calcein, 1,6-diphenyl-1,3,5-hexatriene (DPH), 8-anilino-1-naphthalenesulfonic acid (ANS), and 1-pyrenecarboxaldehyde (PyCHO) were obtained from Sigma−Aldrich Japan (Tokyo, Japan). 1-Ethyl-3-(3-dimethylaminopropyl) carbodiimide (EDC) was obtained from Wako Pure Chemical Industries (Osaka, Japan). Azobis(isobutyronitrile) (AIBN), tris(hydroxymethyl)aminomethane (Tris), *N*,*N*-dimethylformamide (DMF), and ethylenediamineteraacetic acid disodium salt (EDTA) were from Kishida Chemical (Osaka, Japan). NIPAM and AIBN were purified by crystallization from benzene−*n*-hexane and methanol, respectively. APr was prepared as previously reported (*26*). NIPMAM was synthesized according to the method reported by Jordan et al. (*27*). *N*,*N*-Didodecylsuccinamic acid was synthesized according to the method of Okahata and Seki (*28*).

2.2. Synthesis of NIPAM Copolymers with Anchor. Three kinds of NIPAM copolymers having two dodecyl groups at the chain end, $2C_{12}$-poly(APr-*co*-NIPAM), $2C_{12}$-poly(DMAM-*co*-NIPAM), and $2C_{12}$-poly(NIPMAM-*co*-NIPAM) (Figure 1), were prepared according to the method previously reported (*25*, *29*). In brief, for the synthesis of $2C_{12}$-poly(APr-*co*-NIPAM), APr (15.7 mmol), NIPAM (12.8 mmol), 2-aminoethanethiol (0.4 mmol), and AIBN (0.03 mmol) were dissolved in freshly distilled DMF (12 mL) and then the solution was heated at 75 °C for 15 h in N_2 atmosphere. The copolymer was recovered by precipitation with diethyl ether and further purified on a Sephadex LH-20 column eluted with methanol. The obtained poly(APr-*co*-NIPAM) having an amino group (1.5 g) at the terminus was reacted with *N*,*N*-didodecylsuccinamic acid (3.3×10^{-4} mol) in DMF (50 mL) with 1-ethyl-3-(3-dimethylaminopropyl) carbodiimide (3.3×10^{-4} mol) for 48 h at 4 °C. The copolymer having a didodecyl group, $2C_{12}$-poly(APr-*co*-NIPAM), was purified by an LH-20 column eluting with methanol (yield 1.1 g). The $2C_{12}$-poly(DMAM-*co*-NIPAM) was prepared according to the above method. DMAM (2.4 mmol), NIPAM (9.4 mmol), 2-aminoethanethiol (0.5 mmol), and AIBN (0.13 mmol) were dissolved in DMF (7.5 mL) and then the solution was heated at 75 °C for 15 h in N_2 atmosphere. The obtained poly(DMAM-*co*-NIPAM) having an amino group (0.5 g) at the terminal was reacted with *N*,*N*-didodecylsuccinamic acid (1.5×10^{-4} mol) in DMF (15 mL) with 1-ethyl-3-(3-dimethylaminopropyl) carbodiimide (1.5×10^{-4} mol) for 48 h at 4 °C. The copolymer having a didodecyl group, $2C_{12}$-poly(DMAM-*co*-NIPAM), was purified as described above (yield 0.25 g). The $2C_{12}$-poly(NIPMAM-*co*-NIPAM) was synthesized by the same method. NIPMAM (15.7 mmol), NIPAM (19 mmol), 2-aminoethanethiol (1.15 mmol), and AIBN (0. 3 mmol) were dissolved in DMF (20 mL) and then the solution was heated at 75 °C for 15 h in N_2 atmosphere. The obtained poly(NIPMAM-*co*-NIPAM) having an amino group (1.5 g) at the terminus was reacted with *N*,*N*-didodecylsuccinamic acid (3.3×10^{-3} mol) in DMF (50 mL) with 1-ethyl-3-(3-dimethylaminopropyl) carbodiimide (3.3×10^{-3} mol) for 48 h at 4 °C. The copolymer having a didodecyl group, $2C_{12}$-poly(NIPMAM-*co*-NIPAM), was purified as described above (yield 1.1 g).

2.3. Liposome Preparation. The liposomes were prepared as previously reported (*20*, *29*). EYPC in chloroform solution (10 mg/mL, 1 mL) and the copolymer in chloroform solution [10 mg/mL, 1 mL for $2C_{12}$-poly(NIPMAM-*co*-NIPAM) and $2C_{12}$-poly(APr-*co*-NIPAM) or 4 mL for $2C_{12}$-poly(DMAM-*co*-NIPAM)] were mixed in a flask and the solvent was removed by evaporation. The obtained thin lipid/copolymer mixed membrane was further dried under vacuum overnight and dispersed in 1.5 mL of an aqueous calcein solution (63 mM). The obtained liposome suspension was extruded through a polycarbonate membrane with a pore diameter of 100 nm in an ice-cooled water bath. The free calcein and free copolymer were removed by gel-permeation chromatography (GPC) on a Sepharose 4B column at 4 °C in a 10 mM Tris-HCl-buffered solution containing 140 mM NaCl and 1 mM EDTA solution at pH 7.4. The calcein-loaded liposomes were kept at 5 °C until the measurement.

2.4. Calcein Release from Liposome. The release measurements were performed according to the method previously reported (*26*, *29*). An aliquot of dispersion of the calcein-loaded liposomes was added into 2 mL of 10 mM Tris-HCl, 140 mM NaCl, and 1 mM EDTA solution (pH 7.4) in a quartz cell (final concentration of the lipids 10 μM) at a given temperature, and the fluorescence intensity of the solution was monitored on a spectrofluorometer (Shimadzu RF-5000). The excitation and monitoring wavelengths were 490 and 520 nm, respectively. The percent release of calcein from the liposomes was defined as

$$\% \text{ release} = (F^t - F^i)/(F^f - F^i) \times 100$$

where F^i and F^t mean the initial and intermediary fluorescence intensities of the liposome suspension, respectively. F^f is the fluorescent intensity of the liposome suspension after the addition of Triton X-100 (final concentration 0.15%).

2.5. Estimation of the Amount of Copolymer Bound to Liposome. The amount of the copolymer bound to the liposome was estimated by use of high-performance liquid chromatography as previously reported (*24*, *29*). The liposomes bearing the copolymer were dried under vacuum and then dissolved in methanol/water (7:3 v/v). The solution was filtered through a poly(tetrafluoroethylene) membrane with a pore size of 0.25 μm. The filtrate (20 μl) was injected into an SB-803 column (Showa Denko) and the effluent was monitored by the absorbance at 220 nm on a UV detector (Jasco, UV-790). The amount of copolymer was estimated from the absorbance of the separated copolymer. Also, the lipid amount was determined by the method of Bartlett (*30*).

2.6. Fluorescence Measurements. Emission spectra of PyCHO were obtained on a spectrofluorometer with excitation at 365.5 nm. Fluorescence polarization (P) of DPH and ANS was measured as reported previously (*31*). ANS and DPH were excited at 395 and 360 nm, respectively, and the fluorescence intensities of ANS and DPH were monitored at 467 and 428 nm, respectively. The P value was evaluated by use of

$$P = (I_p - I_v)/(I_p + I_v)$$

where I_p and I_v represent the intensities of parallel polarized fluorescence and vertically polarized fluorescence, respectively.

2.7. Other Methods. The size of liposomes was evaluated by dynamic light scattering on a Nicomp 380 ZLS instrument (Particle Sizing Systems). The weight-average molecular weight (M_w) and the number-average molecular weight (M_n) of the polymers were estimated by gel-permeation chromatography on a system equipped with a Shodex KD-803 column (Showa Denko) with differential refractive index detection (Jasco, RI-930) with DMF as an eluent and poly(ethylene glycol) as the standard. Differential scanning calorimetry (DSC) was performed with a DSC 120 microcalorimeter (Seiko Electronics).

3. RESULTS AND DISCUSSION

3.1. Characterization of Copolymer and Copolymer-Modified Liposomes. It is known that the LCST of poly(NIPAM) can be controlled by copolymerization with comonomers having varying degrees of hydrophilicity/hydrophobicity (*32*). In this study, we used three kinds of comonomers, APr, DMAM, and NIPMAM, to obtain NIPAM copolymers that have different structures but exhibit the same LCST. Because the most attractive application of temperature-sensitive liposomes is the drug delivery application, we chose 40 °C as the LCST of the copolymers. Such temperature-sensitive liposomes can deliver drugs by specifically releasing them at the target site, which is mildly heated above that temperature (*2*). APr and DMAM have already been used to obtain NIPAM copolymers with an LCST around the physiological temperature (*26*, *27*).

Copolymerization of NIPAM and these comonomers was performed in the presence of the chain transfer reagent 2-aminoethanethiol to introduce an amino group at one terminus of the copolymer chain (*34*), which can be used for the attachment of a hydrophobic moiety for the fixation of the copolymer chain to the liposome membrane. The compositions of the copolymers were estimated from the integral ratios of signals derived from NIPAM and the comonomer units in the ^{1}H NMR spectra (Figure 2). Also, the number-average molecular weight (M_n), the weight-average molecular weight (M_w), and polydispersity index (M_w/M_n) of the copolymers were evaluated by gel-permeation chromatography with poly(ethylene glycol) as the standard. The results for the copolymers used in this study are listed in Table 1.

The cloud point measurement was performed to determine the LCST of the copolymer before the conjugation of the anchor. Figure 3 shows the transmittance of the aqueous solutions of these copolymers. The solutions were transparent below 38 °C, indicating that these copolymers were soluble in water below 38 °C. However, the solution became turbid around 40 °C, showing that these copolymers became water-insoluble around this temperature. The LCSTs of poly(APr-*co*-NIPAM), poly(DMAM-*co*-NIPAM), and poly(NIPMAM-*co*-NIPAM) were estimated from Figure 3 and are listed in Table 2.

It is known that the LCST of poly(NIPAM) can be determined by DSC (*22*, *35*). Thus, we examined the calorimetric detection of LCST for these copolymer solutions. Figure 4 depicts the typical DSC curves of these copolymer solutions. These curves exhibited an endotherm centered at approximately the same temperature, 40 °C, which agrees well with their LCST determined from the cloud point measurement. However, the amplitude of the endotherm significantly varies among these copolymers. As shown in Table 2, ΔH for the phase separation increases in the order poly(APr-*co*-NIPAM) < poly(DMAM-*co*-NIPAM) < poly(NIPMAM-*co*-NIPAM). Because the endotherm is mainly related to the destruction of water around the hydrophobic groups (*32*), this result suggests that the poly(NIPMAM-*co*-NIPAM) forms

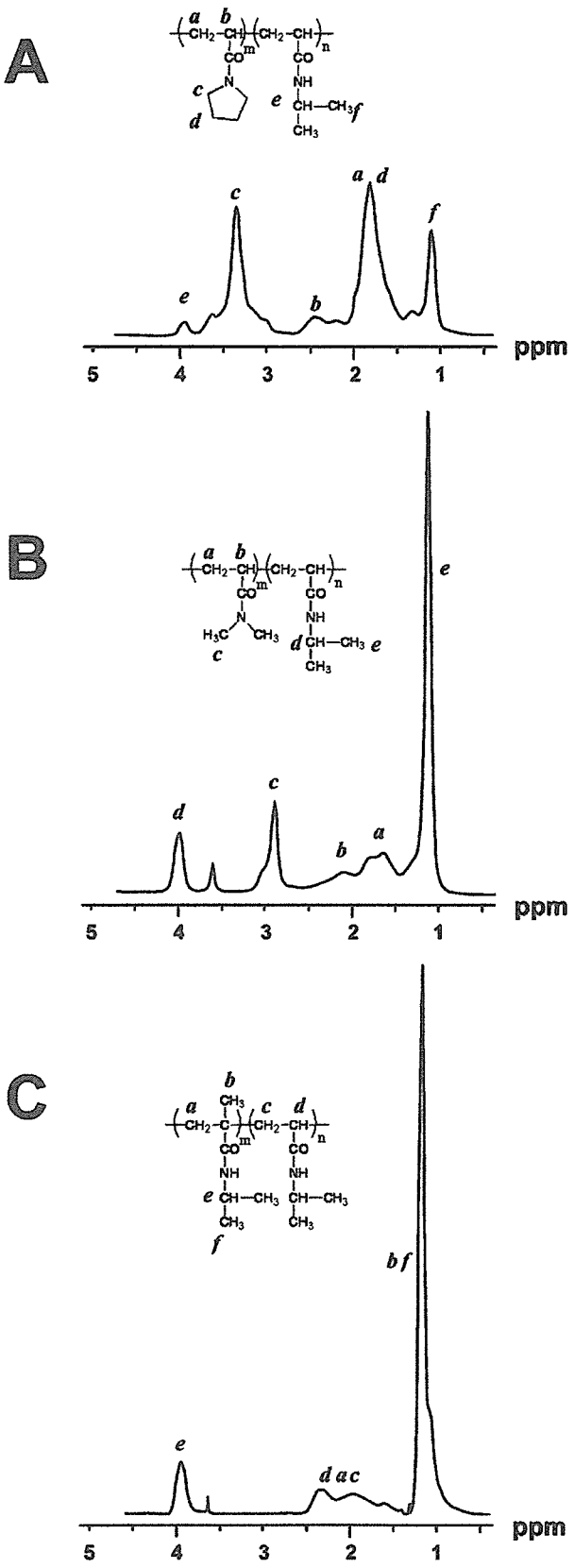

Figure 2. ^{1}H NMR spectra for poly(APr-*co*-NIPAM) (A), poly(DMAM-*co*-NIPAM) (B), and poly(NIPMAM-*co*-NIPAM) (C) in $CDCl_3$.

the most hydrophobic domain above the LCST, whereas poly(APr-*co*-NIPAM) forms the least hydrophobic domain among these copolymers.

Many studies have shown that a variety of hydrophilic polymers with hydrophobic anchor moieties can be fixed

Table 1. Characterization of the NIPAM Copolymers

copolymer	composition[a] comonomer/ NIPAM (mol/mol)	M_n[b]	M_w[b]	M_w/M_n[b]
poly(APr-*co*-NIPAM)	81/19	4100	9200	2.2
poly(DMAM-*co*-NIPAM)	28/72	4600	12800	2.8
poly(NIPMAM-*co*-NIPAM)	46/54	4850	7550	1.6

[a] Estimated by ^{1}H NMR. [b] Estimated by GPC.

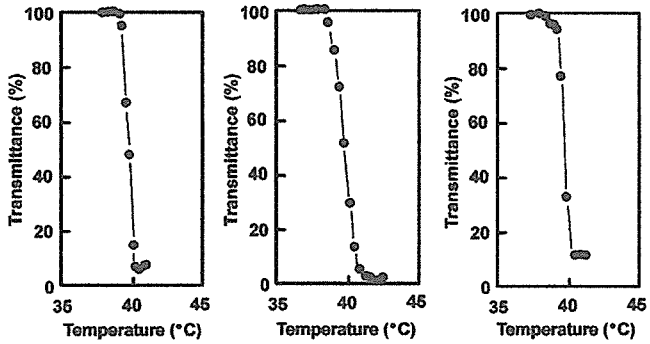

Figure 3. Cloud point curves for aqueous solutions of copoly(NIPAM-APr) (A), poly(DMAM-*co*-NIPAM) (B), and $2C_{12}$-poly(NIPMAM-*co*-NIPAM) (C).

Table 2. LCST of Copolymers

copolymer	cloud point (°C)	T_{max}[a] (°C)	ΔH (J/g)
poly(APr-*co*-NIPAM)	38.6	39.0	1.4
poly(DMAM-*co*-NIPAM)	39.8	41.1	11.8
poly(NIPMAM-*co*-NIPAM)	39.4	39.6	26.8

[a] Temperature of peak maximum of calorimetric endotherm.

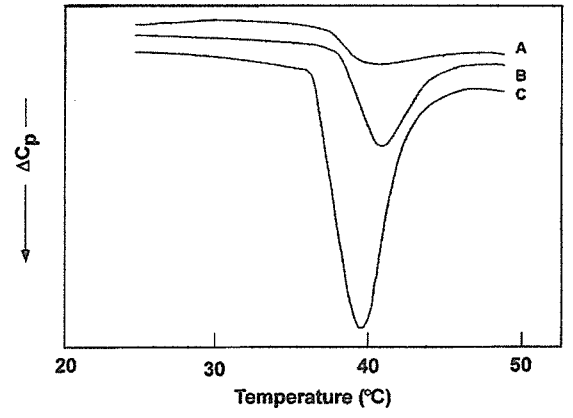

Figure 4. Microcalorimetric endotherms for copoly(NIPAM-APr) (A), poly(DMAM-*co*-NIPAM) (B), and poly(NIPMAM-*co*-NIPAM) (C).

to liposome membranes by a hydrophobic interaction between the hydrophobic moieties and liposome membranes (*12*, *15*, *36*). Since these copolymers have an amino group at one terminus of the chain, two dodecyl groups were introduced to the chain end by reacting didodecylsuccinamic acid with the terminal amino group. We have already shown that the didodecyl group can act as an anchor for the fixation of the NIPAM copolymers to the liposome membranes (*26*, *29*, *31*).

Liposomes modified with the copolymers bearing the anchor, $2C_{12}$-poly(APr-*co*-NIPAM), $2C_{12}$-poly(DMAM-*co*-NIPAM), and $2C_{12}$-poly(NIPMAM-*co*-NIPAM), were prepared by hydration of a mixture of EYPC and the copolymer and subsequent extrusion through a polycarbonate membrane with a pore size of 100 nm. The free

copolymer, which was not bound to the liposome membrane, was removed by GPC. The mean diameters and the standard deviations of the EYPC liposomes modified with $2C_{12}$-poly(APr-*co*-NIPAM), $2C_{12}$-poly(DMAM-*co*-NIPAM), and $2C_{12}$-poly(NIPMAM-*co*-NIPAM) were estimated by dynamic light scattering to be 125.7 ± 1.4, 106.6 ± 11.4, and 95.8 ± 3.8 nm, respectively, at 20 °C. It is apparent that these copolymer-modified liposomes possess diameters close to the pore size of the polycarbonate membrane used to prepare the liposomes. The amounts of the fixed copolymer were found to be 0.66, 0.44, and 0.58 mg/mg of liposomal lipid for liposomes modified with $2C_{12}$-poly(APr-*co*-NIPAM), $2C_{12}$-poly(DMAM-*co*-NIPAM), and $2C_{12}$-poly(NIPMAM-*co*-NIPAM), respectively, indicating that these copolymer-modified liposomes contain similar amounts of the copolymers. As indicated in the Experimental Section, the amounts of $2C_{12}$-poly(APr-*co*-NIPAM), $2C_{12}$-poly(DMAM-*co*-NIPAM), and $2C_{12}$-poly(NIPMAM-*co*-NIPAM) mixed with the lipid (10 mg) were 10, 40, and 10 mg, respectively, for the preparation of the liposomes. Thus, their binding efficiencies are calculated to be 66%, 11%, and 58%, respectively. The contents of the didodecylsuccinamic acid residues in these copolymers were estimated to be 0.6, 0.4, and 1.0 mol %, respectively, from ^{1}H NMR spectra for these anchor-bearing copolymers. Therefore, the low content of the anchor moiety and relatively high polydispersity (Table 1) of $2C_{12}$-poly(DMAM-*co*-NIPAM) may produce the low fixation efficiency.

3.2. Calcein Release from Copolymer-Modified Liposomes. We have already demonstrated that liposomes modified with thermosensitive polymers hardly release their contents below the LCST of the polymer but enhance the contents release above the LCST (*10*, *25*). Figure 5A shows profiles of calcein release from EYPC liposomes modified with these NIPAM copolymers at 25 and 42 °C. As is apparent in Figure 5A, all of the copolymer-modified liposomes did not release calcein at 25 °C. Because these copolymers showed an LCST around 40 °C, this result indicates that well-hydrated chains of these copolymers do not destabilize the liposomal membrane, despite the difference in their molecular structures. In contrast, at 42 °C, an enhancement of the contents release was seen for all of the copolymer-modified liposomes, but the extent of the enhancement was quite different among them. The liposomes modified with $2C_{12}$-poly(APr-*co*-NIPAM) showed only a limited extent of calcein release. However, the liposomes modified with $2C_{12}$-poly(DMAM-*co*-NIPAM) moderately promoted the contents release, and a very rapid and intensive release was observed for the liposomes modified with $2C_{12}$-poly(NIPMAM-*co*-NIPAM).

Figure 5B represents the percent release of calcein from these copolymer-modified liposomes as a function of temperature. For all of the liposomes, the calcein release was enhanced around 40 °C, indicating that the enhancement is triggered by the dehydration of the copolymers above their LCST. For the liposomes modified with $2C_{12}$-poly(APr-*co*-NIPAM), the release gradually increased with increasing temperature above 40 °C. This may be because dehydration of the copolymer chain proceeds with temperature even after its conformational transition. However, even at 50 °C, only 20% of the entrapped calcein molecules were released from the $2C_{12}$-poly(APr-*co*-NIPAM)-modified liposomes. Similarly, for the $2C_{12}$-poly(DMAM-*co*-NIPAM)-modified liposomes, an enhancement in the contents release occurred above 40 °C and the release was promoted by temperature, although the extent of the release was higher than the case

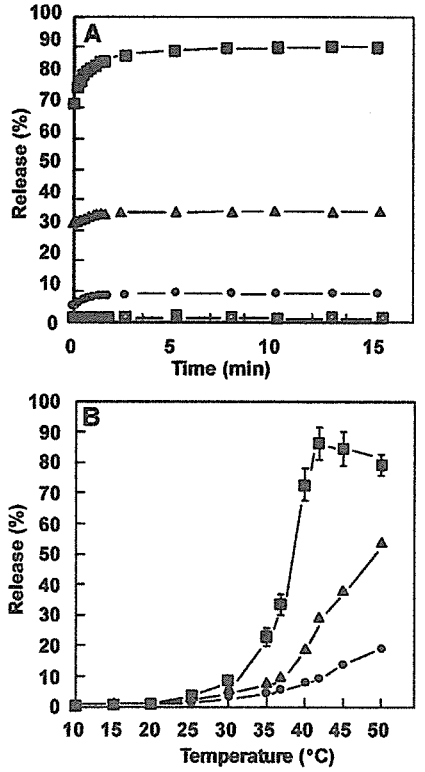

Figure 5. Release of calcein from $2C_{12}$-poly(APr-*co*-NIPAM)-modified (○, ●), $2C_{12}$-poly(DMAM-*co*-NIPAM)-modified (△, ▲), and $2C_{12}$-poly(NIPMAM-*co*-NIPAM)-modified EYPC liposomes (□, ■) in 10 mM Tris-HCl and 140 mM NaCl solution (pH 7.4). (A) Time course of calcein release at 25 °C (open symbols) and 42 °C (solid symbols). (B) Percent release after 15-min incubation as a function of temperature.

of the $2C_{12}$-poly(APr-*co*-NIPAM)-modified liposomes. For the $2C_{12}$-poly(NIPMAM-*co*-NIPAM)-modified liposomes, an intensive promotion of the release is seen around 40 °C, indicating that this copolymer chain strongly destabilizes the liposome membrane when dehydrated. A certain degree of contents release was also observed at 35 and 37 °C, although these temperatures are below the LCST. As seen in Figure 4, the DSC curve for the poly(NIPMAM-*co*-NIPAM) solution exhibits a large endotherm between 35 and 45 °C. This fact indicates that partial dehydration occurs even below the LCST. Thus, it is likely that the dehydrated segments of the copolymer chain interact with the liposome membrane and induce the contents release to some extent (*29*).

As mentioned above, the extent of partitioning of the copolymers onto the liposome increased in the order of $2C_{12}$-poly(DMAM-*co*-NIPAM) < $2C_{12}$-poly(NIPMAM-*co*-NIPAM) < $2C_{12}$-poly(APr-*co*-NIPAM), although the amounts of the bound copolymer were in the range of 0.44−0.66 mg/mg of lipid and not very different among these copolymer-modified liposomes. Therefore, the observed difference in their degree of contents release behavior cannot be explained from the difference in the extent of the copolymer partitioning. Thus, the ability of the dehydrated copolymer chain to induce the contents release could vary depending on their molecular structures.

3.3. Association of Copolymer-Modified Liposomes. Because the surface of the liposomes is covered by the hydrated copolymer chains below the LCST, these copolymer chains would enhance hydration of the liposome surface. However, above the LCST, dehydration of the copolymer chains would cause binding of the dehydrated copolymer chains onto the liposome surface,